



SRC

CHIMIE

143

NOUVELLE

LA REVUE DE CONTACT DE LA SOCIÉTÉ ROYALE DE CHIMIE

41^{ème} année - décembre 2023

SRC
SOCIÉTÉ ROYALE DE CHIMIE

Theoretical **attochemistry**

- Investigation of Ultrafast Phenomena in Attochemistry using Singular Value Decomposition** 1
M. BLAVIER

Frustrated Lewis pair chemistry

- Frustrated Lewis pair chemistry: early concepts, scope, and recent developments with 9-phosphatriptycenes** 15
D. MAHAUT, B. CHAMPAGNE, and G. BERIONNI

Rubrique de la SRC

- Nouvelles de la division des Jeunes Chimistes de la SRC** 39
Echos de la Journée scientifique de la SRC 2023 43
La SRC a un nouveau logo... 43

Directeurs de rédaction

Bernard Mahieu
UCLouvain, Ecole de Chimie
Place Pasteur, 1
Boite L4.01.07
1348 Louvain-la-Neuve
bernard.mahieu@uclouvain.be

Benoît Champagne
UNamur,
Département de Chimie
Rue de Bruxelles, 61
5000 Namur
benoit.champagne@unamur.be

Cédric Malherbe
ULiège,
Département de Chimie
Quartier Agora,
allée du six Août 11
4000 Liège 1
c.malherbe@uliege.be

Infographisme

emmanuel@norproduction.eu

Comité de rédaction

Kristin Bartik, ULB
Nicolas Blanchard, Université de Haute-Alsace-Université de Strasbourg
Sophie Carencio, Sorbonne Université, Paris
Frédéric Castet, Université de Bordeaux
André Colas, Dow Corning
Damien Debecker, UCLouvain
Karolien De Wael, UAntwerpen
Philippe Dubois, UMONS
Anne-Sophie Duwez, ULiège
Gwilherm Evano, ULB
Danielle Fauque, Université de Paris Sud
Stéphane Gérard, Faculté de Pharmacie, Reims
Bernard Joris, ULiège
Sophie Laurent, UMONS
Tatjana Parac-Vogt, KU Leuven
Raphaël Robiette, UCLouvain
Cédric Samuel, École des Mines de Douai
Armand Soldera, Université de Sherbrooke
Johan Wouters, UNamur

Secrétariat

Violaine SIZAIRE
ULB
avenue Franklin Roosevelt 50, CP 160/07 1050 Bruxelles
Tel : +32 2 650 52 08 Fax : +32 2 650 51 84 - email : src@ulb.be
Fortis : BE60 2100 4208 0470

Comité directeur

Conseil de gestion

Présidente	A.-S. Duwez, ULiège	asduwez@uliege.be
Vice-président	J.-P. Lecomte, DOW	j.lecomte@dow.com
Président sortant	L. Provins, UCB	laurent.provins@ucb.com
Secrétaire générale	C. Buess-Herman, ULB	Claudine.Buess-Herman@ulb.be
Trésorier	P. Laurent, ULB	Pascal.Laurent@ulb.be
Délégué relations extérieures	P. Baekelmans, Solvay	paul.baekelmans@solvay.com

Divisions

Chimie Médicinale	L. Provins, UCB	laurent.provins@ucb.com
Chimie organique et bio-organique	M. Larry, ULiège	max.larry@uliege.be
Jeunes Chimistes	T. Massenet, ULiège	thibault.massenet@uliege.be
Histoire et Enseignement de la Chimie	B. Van Tiggelen	vantiggelen@memosciences.be
Délégué Essenscia Wallonie	C. Moucheron, ULB	Cecile.Moucheron@ulb.be
	T. Randoux, Certech	Thierry.Randoux@certech.be

Sections locales

Bruxelles	G. Evano, ULB	Gwilherm.Evano@ulb.be
Louvain-la-Neuve	B. Elias, UCLouvain	benjamin.elias@uclouvain.be
Mons	P. Gerbaux, UMONS	pascal.gerbaux@umons.ac.be
Liège	A. S. Duwez, ULiège	asduwez@ulg.ac.be
Namur	J. Wouters, UNamur	johan.wouters@unamur.be

Membres protecteurs de la SRC

ALLNEX
CERTECH
EXXONMOBIL CHEMICAL
LHOIST
SOLVAY
TOTALENERGIES
UCB

Parution : trimestrielle

Avec le soutien du Fonds National de la Recherche Scientifique.
Les articles paraissant dans Chimie nouvelle sont repris dans CHEMICAL ABSTRACTS

Editeur responsable : Claudine Buess-Herman,
ULB, CP 160/07,
avenue Roosevelt 50, 1050 Bruxelles

Les articles sont soumis à un processus de reviewing.
Les annonces publicitaires sont établies sous la responsabilité des firmes.

« CHIMIE NOUVELLE » est un titre déposé

ISSN 0771-730X

Martin BLAVIER¹¹Theoretical Physical Chemistry, UR MOLSYS,
University of Liège, 4000 Liège, Belgium

*Phone Number: +32 494 26 99 65,

Email Address: martin.blavier@uliege.be,Present address: NANOCHEM, UR MOLSYS,
University of Liège, 4000 Liège, Belgium

Investigation of Ultrafast Phenomena in Attochemistry using Singular Value Decomposition

The following article describes results in the field of (theoretical) attochemistry, a recent discipline focused on the effects of ultrafast (less than a femtosecond) optical pulses on molecular systems and the discovery of potentially new and exotic reaction pathways. This discipline would not have appeared without the creation of the field of attosecond physics, whose breakthroughs allowed the understanding and the creation of such ultrafast optical pulses. Attosecond physics have recently made the news, as this year Pierre Agostini, Ferenc Krausz and Anne L’Huillier were awarded the Nobel Prize in Physics “for experimental methods that generate attosecond pulses of light for the study of electron dynamics in matter”. [1] In that regard, this article proves to be in the spirit of the times.

Abstract

In attochemistry, attopulses are used to initiate chemical reactions. The intrinsically coherent molecular dynamics which arises from the

interaction of matter with ultrashort pulses might lead to new synthetic possibilities. The experimental study of attochemical phenomena is, however, a difficult task which relies on theoretical models to obtain insights in the effects at play. These theoretical models are nevertheless also difficult to set up and the subsequent analysis of the data is rarely straightforward. Therefore, any method that might simplify the creation of a suitable theoretical model of a system or the analysis of the data produced is useful. In this article, one such method, the singular value decomposition, is considered. The handiness of this decomposition is then exemplified with two different examples: the study of the isotope effect in the Jahn-Teller rearrangement of the methane cation and the analysis of the evolution of the entanglement in the photoexcitation of lithium hydride.

Keywords: Attochemistry, Singular Value Decomposition, Entanglement, Molecular Quantum Dynamics

[1] *The Nobel Prize in Physics 2023*. NobelPrize.org. <https://www.nobelprize.org/prizes/physics/2023/press-release/> (accessed 2023-11-07).

1. Introduction

Along with the familiar paradigm of thermal chemistry, another most common activation method is photochemistry, where the energy used to activate chemical bonds and induce chemical reactions arises from electromagnetic radiations. The history of photochemistry begins long before the idea of chemistry and even mankind first appeared, displaying crucial roles in the early synthesis of organic compounds or in complex biological reactions such as photosynthesis. But photochemistry proves to be important for more than those natural examples and display an accrued interest for its synthetic possibilities [1].

On a fundamental point of view, even more promising possibilities have been made available recently due to advances in attosecond science [2], opening the door for the emergence of the field of attochemistry. In attochemistry, ultrashort optical pulses are used to excite specifically electronic motion before the onset of nuclear motion, allowing for the observation and possibly the control of the electronic density on its own time scale, the attoscale (10^{-18} – 10^{-15} s) [3-6].

Because of their extremely short duration, attopulses are characterized by a broad energy bandwidth, which can be resonant with several electronic states of a molecule, leading to the formation of a coherent superposition of electronic states in the initial state of the quantum dynamics. These intrinsically coherent electronic dynamics on a superposition of electronic states are an essential feature of attochemistry, separating it with the closely related field of femtochemistry [7], in which a single electronic state is populated and the electronic dynamics only show a coherent character when electronic states are close in energy (for example near avoided crossings or conical intersections) and not from their very beginning. This difference in dynamics might provide an access to new chemical reactions, allowing either to obtain new compounds or discover new pathways to create already known ones. These newfound synthetic possibilities show much promise for attochemistry.

Attochemical experiments are nevertheless burdened by the inherent complexity of the data obtained, in part due to the coherent character of the dynamics. The accurate and comprehensive interpretation of the results remains a heavy task and, in many cases, a theoretical model of the underlying molecular quantum dynamics is necessary to provide insights to the experimental data.

The setting up these theoretical models is nevertheless no bed of roses, as the highly coherent dynamics exhibited in attochemistry require a suitable description of electronic coherences, that is, interference effects between several electronic states. In this article, the molecular dynamics of the system considered were computed using a fully quantum method, which allows for a full description of the electronic coherences. However, this method proves to be computationally intensive for all systems, even small molecules like CH_4 , as it suffers from the curse of dimensionality [8]: the computational cost scales exponentially with the number of degrees of freedom in the system. Here, the degrees of freedom considered are of vibrational and electronic nature.

This high computational cost thus motivates the use of algebraic methods to either decrease the complexity of the quantum computations or to allow a simpler or different insight into the large amount of data obtained from the theoretical models might prove invaluable. One such algebraic method is investigated here: the singular value decomposition (SVD). The SVD is an algebraic decomposition widely used in statistics and genomics to either decouple in a given matrix two degrees of freedom of different nature or to extract the best few-rank approximation of this matrix. Those two approaches prove to be of interest for the study of attochemical phenomena, as it will be exemplified for **two different applications**: first by the study of the isotope effect in the ultrafast Jahn-Teller rearrangement of the methane cation (CH_4^+) and then by the study of the evolution of the entanglement in the photoexcitation of lithium hydride (LiH). These

two systems were described on a grid of nuclear geometries in order to compute their quantum dynamics.

This article will first consist of a theoretical review of the concepts behind molecular quantum dynamics on a grid and the singular value decomposition, followed by a short description of the results obtained through these techniques on the molecules of interest.

Box 1. Coherent Dynamics

A quintessential feature of quantum mechanics is the superposition principle, which states that given two states of a system, the sum (superposition) of the two states gives another valid state for the system of interest. The probability density given by the square modulus of such resulting state is then more complex than simply the (weighted) sum of the probability density for each state, and interference effects appear. These interference effects also impact the time evolution of the resulting state, as it cannot be an eigenstate of the Hamiltonian operator. [9]

In quantum chemistry, the electrons are described using electronic states, which are the eigenstates of the electronic Hamiltonian operator [10]. By the superposition principle, a sum of several electronic states is another valid initial state for the electronic motion, but the probability density for the resulting state and its time evolution will display interference effects between one electronic state and another, resulting in so-called coherent ("interfering") dynamics between electronic states. This coherent superposition of electronic states can be produced either directly by the photoexcitation of a molecule with a large energy-bandwidth optical pulse, such as an attopulse, or during the molecular dynamics through non-adiabatic couplings, which will be discussed later.

2. Theory

2.1. Quantum molecular dynamics on a grid

In order to describe the quantum dynamics of the molecular systems we wish to study, we must solve numerically the Time Dependent Schrödinger Equation (TDSE).

$$i\hbar \frac{\partial \psi}{\partial t} = \hat{H}(t)\psi, \quad \psi(t_0) = \psi_0 \quad 1.1.$$

Two important quantities must be provided in the previous equation: the Hamiltonian operator associated with the system $\hat{H}(t)$ and the initial state of the system Ψ_0 . To this end, the possible states of the system (three coordinates for each electron and each nucleus in the molecule) must be discretized. In order to simplify the computations, the Born-Oppenheimer approximation is used, an approximation which considers that one can decouple the motion of the electrons and the nuclei because of their difference in mass for each geometry of the nuclei. This approximation allows the computation of adiabatic electronic potentials for the molecule. These potentials, along with the Coulomb repulsion of the nuclei, constitute effective potentials in which the nuclei move.

This leads to a considerable reduction in the degrees of freedom to take into account in the molecular dynamics, as the electronic degrees of freedom are decoupled from the nuclear ones. However, this decoupling is approximate since the electronic states resulting from the BO approximation are coupled by non-adiabatic interactions driven by the nuclear motion (see below), and the number of coupled electronic states can be large as the dynamics unfolds. Moreover, this is not sufficient, as the discrete description of the remaining nuclear degrees of freedom scales exponentially with the number of nuclear coordinates to account for. Currently, grid-based molecular dynamics on several coupled electronic states involving more than three nuclear coordinates prove to be intractable. In the case of non-linear molecules, this leads therefore to the need of reducing the dimensionality of the problem even further by

restricting the model to the appropriate nuclear coordinates for the description of the dynamics.

Only then can we begin to describe the state space of the system as a grid of several orthogonal grid points, representing each a different nuclear geometry and to which different electronic states are associated. The wavefunction of the system will thus be described as sum of product terms made of a complex amplitude associated with each grid point and each electronic state, amplitude denoted c_{gi} . The set of all these amplitudes then consists of an amplitude vector c . This is represented visually in figure 1, which shows the grid points which are coupled due to the non locality of the kinetic energy and momentum operators represented in a finite difference approximation for two nuclear coordinates [11]. The structure of the kinetic energy and momentum operator in the system of coordinates used in [11] is also depicted.

The choice of this basis for the nuclear wavefunction allows us to express the nuclear Hamiltonian operator which will act on the amplitude vector in a matrix form. Its elements are given by expression (1.2)

$$= \mathbf{V}_{gi,g'j} \delta_{gg'} \delta_{ij} + (\mathbf{T}_N)_{gi,g'j} \delta_{ij} (g) \delta_{gg'} - (\mu_{ij}(g) \delta_{gg'}) \cdot \mathbf{E}(t) \quad 1.2.$$

In equation (1.2), $V_{gi,g'j} \delta_{gg'} \delta_{ij}$ is the potential energy operator of the system, which is given as the potential energy surface of a given electronic state at a given grid point. This operator is both diagonal on the grid and on the electronic states.

T_N is the nuclear kinetic energy operator, which is represented in figure 1. for a grid of two nuclear coordinates. The μ are the reduced masses of the system according to the different coordinates considered. This operator does not act on the adiabatic electronic states and thus is diagonal on the electronic states. The nonlocal character of the second order derivative with respect to the nuclear coordinate is approximated as finite differences on the grid, allowing for a numerical resolution of the TDSE [12].

In Eq. (1.2), $\tau_{ij}(g)$ are the derivative couplings between two different electronic states at a given grid point. They are given by electronic structure computations and diagonal on the grid. Along

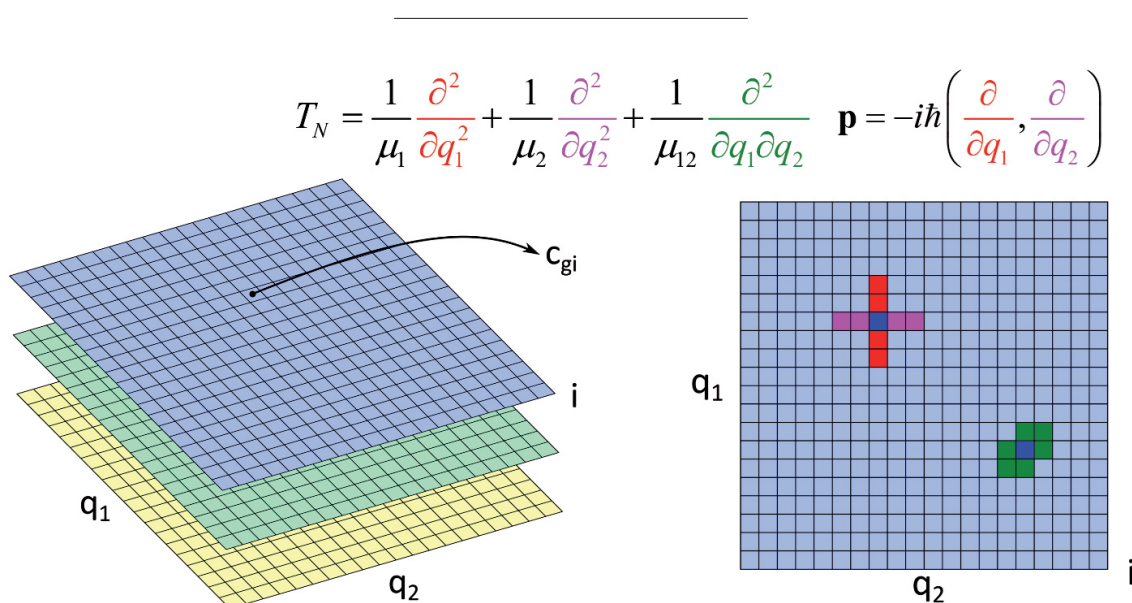


Figure 1: Grid description of the molecular system for the dynamics. q_1 and q_2 are two different nuclear coordinates, whereas the plane i describes the i -th electronic state. On the right, the structure of the kinetic energy and momentum operator on the grid are represented in the framework of finite differences [11, 12].

with the momentum operator $P_{gi,gj}$, they describe non-adiabatic couplings between the electronic states which result from a breakdown of Born-Oppenheimer approximation. The momentum operator $P_{gi,gj}$ is similar in structure to the nuclear kinetic energy term as it is diagonal on the electronic states and the nonlocal property of its first derivative is also approximated using finite differences. It is also represented in figure 1 for a grid of two nuclear coordinates.

The non-adiabatic couplings described by the derivative couplings and the momentum operator arise from the coupling of the motion of the electrons and the nuclei and essentially represent a breakdown of the Born-Oppenheimer approximation. These couplings are the strongest when different electronic potentials are close in energy. They play a crucial role in photochemistry, as it will be shown in the study of the methane cation and the photoexcitation of LiH.

Box 2. Non-adiabaticity

The Born-Oppenheimer approximation allows to decouple the motion of the electron and the nuclei in a molecule. This approximation is motivated by the larger mass of the nuclei compared to the electrons, leading to different time scales for their respective motions and to adiabaticity (decoupling between the motion of the light particles and the heavy particles). It was initially devised by Max Born and J. Robert Oppenheimer [13] to describe the ground state of molecules, which is most of the time well-separated in energy from the excited electronic states and for which this approximation is justified. However, it breaks down as soon as the spacing between several electronic states become close to the spacing between vibrational states, that is, when a coupling between

electronic and nuclear motions becomes possible [14]. This is especially the case near conical intersections, where two or more adiabatic electronic states cross, or avoided crossings, if the electronic states do not ultimately cross but are in close vicinity. These non-adiabatic, or vibronic, couplings lead to the transfer of amplitudes between several electronic states, thereby adding complexity to the quantum dynamics and possibly changing the coherent superposition of the electronic states.

Finally, the interaction with the electric field of an exciting pulse depends on both the permanent $\mu_{ii}(g)$ and transition $\mu_{ij}(g)$ dipole moments for the electronic states, which are also given by electronic structure computations at a given grid point, and thus which are diagonal on the grid. In the case of the photoexcitation of , the electric field of the exciting pulse is described by equation (1.3). It is modelled by a Gaussian envelope centred around t_0 with a standard deviation specifying the length of the pulse. The carrier frequency of the pulse is given by ω and the carrier-envelope phase (CEP) is ϕ . The maximal amplitude of the pulse is given by $|E_0|$. The term $-\frac{\sin(\omega t + \phi)(t - t_0)}{\omega \sigma^2}$ is present in the expression of the pulse to ensure that it remains Fourier-limited even for few-cycle pulses [15].

Thanks to the diagonal character of many operators involved in the Hamiltonian matrix as well as the use of finite difference approximations for the first and the second derivatives with respect to nuclear coordinates, a lot of elements of the Hamiltonian matrix (1.2) are zero and the Hamiltonian matrix is referred to as a “sparse” matrix. The several common linear algebra operations, such as matrix-vector multiplication, can be tailored to take advantage of the sparse structure of the matrix and perform more efficiently the desired operation.

$$\mathbf{E}(t) = |E_0| \hat{\mathbf{e}} \exp\left(-\frac{(t - t_0)^2}{2\sigma^2}\right) \left(\cos(\omega t + \phi) - \frac{\sin(\omega t + \phi)(t - t_0)}{\omega \sigma^2}\right) \quad 1.3.$$

In the case of the propagation of the TDSE (1.1), the nuclear wavefunction is written as a vector of coefficients c_{gi} on the grid, and matrix-vector multiplication of the Hamiltonian matrix (1.2) on the wave vector is performed.

In order to compute the quantum dynamics of the molecular system, we still require an initial state. The choice of this initial state will depend on the phenomenon that is under study. In the first example we will describe, our interest lies in the study of the dynamics occurring in the methane cation produced by high-harmonic spectroscopy (HHS) [16]. This leads us to compute the initial states that arise in HHS. In the second example, the study of the entanglement in the photoexcitation of LiH, the initial state was chosen to be the lowest vibrational state of the ground electronic state. This choice is sensible as the lowest vibrational state is the only populated state in this molecule at room temperature.

The TDSE (1.1) is then numerically integrated at each time step using the Hamiltonian matrix and the initial state previously described in order to express the time evolution of the system. A numerical integration is here necessary as the molecular Hamiltonian, containing the interaction with a time-dependent optical pulse, is time-dependent. This integration is carried out using a fourth-order Runge-Kutta procedure, widely used for solving numerically first-order differential equations.

2.2. Singular value decomposition

The singular value decomposition (SVD) is an algebraic decomposition of matrices with important applications in statistics, signal processing and genomics [17-20]. The importance of this decomposition arises from its universality: all matrices, especially rectangular ones, can be decomposed by SVD.

Mathematically ([21]), let A be a rectangular complex-valued matrix of dimensions $M \times N$, with $M > N$ (the case would simply produce the adjoint of the following expressions). Then this matrix admits a decomposition in the form

(the notation V^\dagger ; means taking the Hermitian conjugate of the matrix V):

$$\mathbf{A} = \mathbf{U}\mathbf{\Sigma}\mathbf{V}^\dagger \quad 1.4.$$

With U a rectangular $M \times N$ matrix whose columns are the *left singular vectors* of A , that is the normalized eigenvectors corresponding to the non-zero eigenvalues of the square matrix AA^\dagger ; Σ the square $M \times N$ matrix containing the *singular values* of A , that is the square roots of the non-zero eigenvalues of both AA^\dagger and $A^\dagger A$ (which importantly have the same eigenvalues but different eigenvectors); V the square $M \times N$ matrix whose columns are the *right singular vectors* of A , *i.e.* the normalized eigenvectors of the non-zero eigenvalues of $A^\dagger A$. In most cases, the singular vectors are complex-valued, whereas the singular values are always real. This decomposition is called the (compact) singular value decomposition of A .

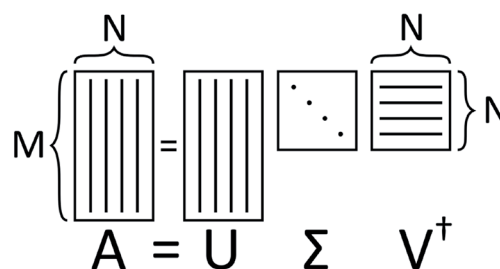


Figure 2: Illustration of the singular value decomposition

The SVD also allows to express the matrix A as a sum of rank-one matrices $u_i v_i^\dagger$:

$$\mathbf{A} = \sigma_1 \mathbf{u}_1 \mathbf{v}_1^\dagger + \sigma_2 \mathbf{u}_2 \mathbf{v}_2^\dagger + \sigma_3 \mathbf{u}_3 \mathbf{v}_3^\dagger + \dots = \sum_{i=1}^R \sigma_i \mathbf{u}_i \mathbf{v}_i^\dagger \quad 1.5.$$

With $R \leq N$ the rank of A . The singular values are given in decreasing order in expression (1.5). If we stop the sum in this expression at a given rank R' , the matrix obtained constitutes the best rank R' approximation of A . This provides with a way to reduce efficiently the rank of a matrix in the hope of simplifying the subsequent computations using that matrix. The first elements of this decomposition describe the broad features of the original matrix A , whereas the last elements of the series describe extremely localized features. By analogy with the

application of SVD to images, we can say that the terms associated with the greatest singular values represent low frequency components of the original matrix, whereas the last terms describe the high frequency components of A .

The first use of SVD in this work builds upon the work of Gonçalves et al. [11], in which the ultrafast dynamics of the methane cation excited by photoionization were computed. In order to create an initial state representative of the ones created in a typical experiment, in which the molecules are randomly oriented with respect to the direction of the electric field, it is more efficient computationally to fix the orientation of the molecule in the molecular frame and randomize the orientation of the exciting electric field with respect to the molecule, each direction leading to a different initial state. This means that in order to reproduce the results of experiments with molecules in a random orientation compared to the laboratory frame, it would be necessary to perform the dynamics on a large number of initial states produced from a random orientation of the electric field, and then study the average effect. Depending on the accuracy required to emulate the experimental conditions, a few thousands of those randomly oriented molecules might be necessary, thereby adding a large cost to the computations. Gonçalves et al. [11] reports another strategy to reduce the number of computations needed to construct a representative initial state for the photoionization of the methane cation: after having produced the set of randomly sampled initial states, the most significant features of this dataset are uncovered using SVD. They then proved that this reduces to only three non-zeros singular values and three associated singular vectors that, together, fully reproduce the features of the complete dataset. It is then sufficient to perform the dynamics on only the three singular vectors, instead of a few thousands of initial states, and then weigh the results obtained by the singular values to describe accurately the dynamics of a sample of randomly oriented molecules. This proves to yield good agreement with the experimental results of Marangos et al. [22].

In a similar spirit, the first part of my master thesis consisted in the study of the ultrafast Jahn-Teller

effect in the methane cation, this time produced by strong field ionization. The initial state for the methane cation is again dependent on the orientation of the exciting electric field, and a similar need for an initial state representative of a sample of randomly oriented molecules is present. A similar strategy as in the case of the photoionization was thus performed. Contrary to photoionization, more than three singular values were required to fully describe the features of the dataset but taking only three proved to be sufficient to explain more than 99.5% of those features. The results obtained were then also in good agreement with the findings of Marangos et al. [22]. More information on this approach can be found in Blavier et al. [23].

The second use of SVD also relied on its property that singular vectors are obtained for both the column space and the row space of the matrix, providing information on the two different types of degrees of freedom described by the initial matrix. The amplitude vector \mathbf{c} may be interpreted as a matrix connecting electronic and nuclear degrees of freedom, and SVD leads to a characterization of those two contributions separately, allowing to study the interplay between those degrees of freedom and even their entanglement. In this way, the SVD allows the computation of the Schmidt decomposition of the state of the system, a decomposition which provides a direct measure of the entanglement of a system through its rank. [24] The connection between SVD and the Schmidt decomposition, as well as the transformation of the amplitude vector in a suitable form is treated in more details in Blavier et al. [25].

Box 3. Entanglement

The concept of entanglement is another feature which is essential to quantum mechanics and often leads to non-intuitive effects. It is defined between two or more interacting systems on which it is possible, at least in theory, to make measurements separately. Entanglement arises from the fact that some (quantum) states from the overall system ($A + B$) cannot be described by the tensor product of states from the

subsystems (states from A and from B). One usual example is the Bell state for a system of two qbits $\frac{1}{\sqrt{2}}(|^{00}\rangle+|^{11}\rangle)$ which cannot, in any way, be expressed as the product of the states of one qbit ($|^0\rangle$ or $|^1\rangle$). The states that can be separated into different states of the subsystems are called separable states, whereas the others are entangled states. [26]

The problem of computing and characterizing the entanglement of a given quantum state is still an ongoing topic of investigation in quantum physics [27]. One simple criterion for bipartite system (a quantum system composed of two subsystems) consists of the Schmidt rank for the state, which is the minimum number of separable terms in the Schmidt decomposition of the state. For a separable state, the Schmidt rank is 1, whereas a Schmidt rank greater than or equal two depicts an entangled state. This is this property of the Schmidt decomposition which allows to characterize the entanglement observed in molecular quantum dynamics [24, 26].

3. Results and discussion

3.1. Strong Isotope effect on the ultrafast Jahn-Teller Rearrangement of the methane cation

The first part of this work was devoted to the study of the Jahn-Teller rearrangement in the methane cation upon strong-field ionization, that is, the observed loss of symmetry of the CH_4 molecule when it is excited by a strong electric field, leading to high-harmonic generation. The harmonics produced can then be studied in order to better understand the quantum dynamics at play, a type of experiments call high-harmonic spectroscopy (HHS).

As said previously, this part built upon the previous work of Gonçalves et al. [11], who already investigated this effect in a molecular

system excited by a short extreme UV optical pulse. The work began by the construction of the Hamiltonian operator associated with this system and was followed by the computation of initial states representative of the state produced by strong-field ionization of system to study the molecular dynamics.

This is where SVD crucially comes into play: as described earlier, SVD can be used to compute a low-rank approximation to any given matrix. A matrix composed of the amplitudes of 8000 random orientations of the exciting electric field was computed and then decomposed, which gave us access to the common features observed for all the different orientations, thereby reducing the task of computing the dynamics of 8000 initial states to only 3 which reproduce more than 99.5% of the features of the original matrix. This significant reduction in computational complexity of the problem allowed us to study the short-time dynamics of the Jahn-Teller rearrangement of CH_4^+ , and characterize the isotope effect and the impact of the strength of the exciting electric field on the coherent dynamics.

For that purpose, two different values for the strength of the electric field were considered: a high value of 2×10^{14} W/cm², commonly used in high-harmonic spectroscopy experiments and referred to in the rest of this manuscript as strong field, and a lower value of 3.16×10^{13} W/cm², denoted as weak field. Computations were performed for both CH_4^+ and CD_4^+ . The resulting electronic populations and electronic coherences are shown in figure 3.

As one can see, in both cases a coherent superposition of electronic states was created, with all electronic states being populated at the onset of the dynamics for both strengths of the electric field. Intuitively, a lower value of the strength led to a smaller population in the excited electronic states (D1 and D2) as the ionization potential of those electronic states was less modified by the weaker exciting electric field. The electronic populations are, however, similar between the two isotopomers of CH_4^+ . A clearer

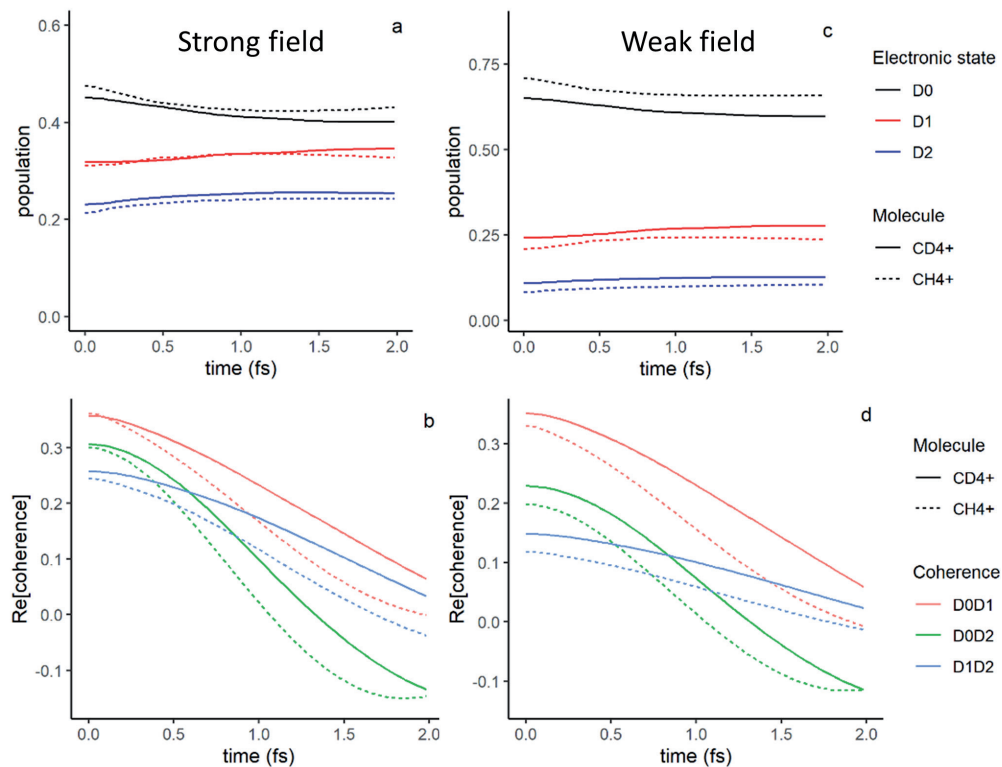


Figure 3: Electronic populations (a, c) and real part of the electronic coherences (b, d) at short times, for respectively the strong field (left) and the weak field (right)

difference can be observed in the real part of the electronic coherences. The oscillations of the coherence are slower in the case of CD_4^+ as the highest mass of the molecular system leads to a slower motion of the wave packets on the electronic states. The electronic coherences therefore prove to be more sensitive to the isotope effect than the populations.

One of the aims of this study was to understand the isotope effect observed experimentally in the yield in harmonics obtained during a HHS experiment, as reported by Marangos et al. [22] This can be assessed theoretically by studying the evolution of the autocorrelation function $|C(t)|^2 = \psi(0) \cdot \psi(t)$, which has been shown to be proportional to this yield in harmonics [29].

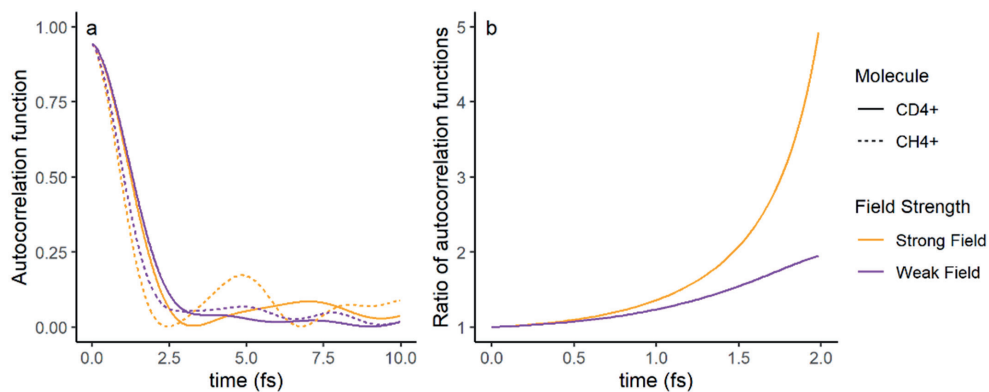


Figure 4: Autocorrelation function (a) and ratio of the autocorrelation functions (b) between CD_4^+ and CH_4^+

The ratio in the autocorrelation functions for CH_4^+ and CD_4^+ can therefore be compared with the ratio of the yields in harmonics obtained. As shown in figure 4, this ratio has been found to be approximately 2.4 at 1.6 fs in the case of the strong field, which is in agreement with the values found experimentally.

One crucial remark to make on this result is that the isotope effect observed in the ratio of the autocorrelation functions is greater than the one simply induced by the difference in mass of the two isotopomers. It mainly arises from the impact of the non-adiabatic couplings between the D_2 state and the others, leading to different dynamics at short times. This highlights the effects that non-adiabatic couplings can have on molecular quantum dynamics.

More information on this work can be found in the article Blavier et al. [23], as the aim of this section was to illustrate the handiness of SVD to reduce the computational cost of the quantum dynamics. Another aspect of this usefulness will now be exemplified with the characterization of the entanglement between electronic and nuclear degrees of freedom in the LiH molecule.

3.2. Analysis of the entanglement within the LiH molecule

To understand the insights that SVD can provide on the interactions between electronic and nuclear degrees of freedom, the choice was made to consider a simpler system than the methane cation, namely lithium hydride (LiH). This molecule is a linear diatomic molecule with a single nuclear degree of freedom, the internuclear distance R . The photoexcitation of this molecule by a few fs deep-UV pulse was then computed, a photoexcitation which led to the creation of a coherent superposition of electronic states and thus to coherent nuclear dynamics. Among the six excited electronic states considered in the dynamics, the most populated by the pulse were the Σ_2 and Σ_4 states. Of all the electronic states that were resonant with the optical pulse, those two indeed possess a stronger transition dipole moment, explaining the difference in population

shown in figure 5.

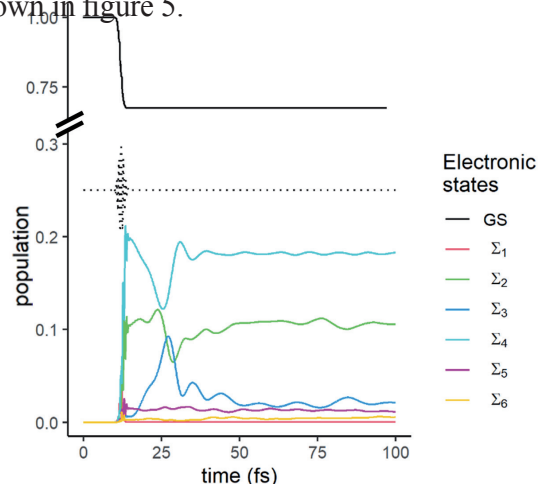


Figure 5: Population of the Σ_2 , Σ_3 and Σ_4 electronic states through time. Note the break in the y axis separating the population of the ground state from the rest. The exciting optical pulse is represented as a black dotted line. Reproduced from Ref. [25] with permission from the PCCC Owner Societies.

As one can see from figure 5, the Σ_2 , Σ_3 and Σ_4 electronic states exhibit the strongest population transfers through time and are the most interesting for the analysis of the electronic coherence. This is because of the strong non-adiabatic couplings that take place between those three electronic states.

The first parameter given to us by the singular value decomposition that we can analyse is the singular values. Drawing from the analogy between the Schmidt decomposition of a quantum system and the SVD, we can infer that if only one singular value is needed for the description of our molecular system at a given time, the system is in a separable state at that time. The evolution through time of the singular values is represented in figure 6.

As one can see, before the onset of the exciting optical pulse, the system lies in a separable state described only by one singular value, which is intuitive as all the electronic wave packet is located on the ground state of the molecule. As soon as the optical pulse creates a coherent superposition of electronic states, at least two singular values are required to describe the state of the system. The coherent excitation of the pulse thus leads to an increase of the entanglement of the state of the molecular

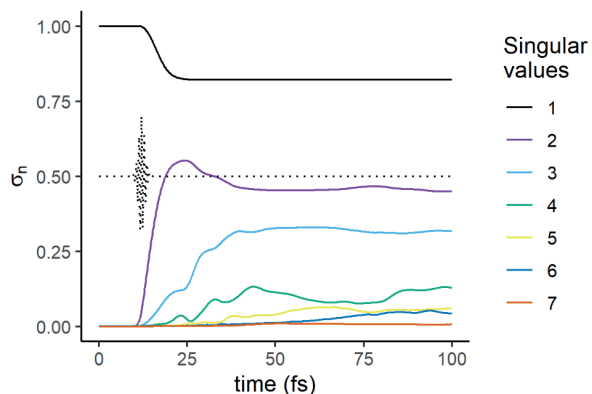


Figure 6: Evolution through time of the singular values. The exciting optical pulse is represented in black. Reproduced from Ref. [25] with permission from the PCCP Owner Societies.

system. An important note has to be made here: the creation of a coherent superposition of electronic states is not a sufficient condition for an increase in the entanglement. Indeed, if all the electronic states possessed the same potential energy surfaces, and thus the same gradient, the motion of the wave packets on each electronic state of the superposition would be identical, leading to a separable state as only one nuclear state is required to explain the motion of all the electronic wave packets.

The previous remark introduces the importance of the difference in the gradients on different electronic states to produce an increase in the entanglement of the system. It also allows us to understand the dynamics of the singular values in figure 6. Indeed, at the maximum of the pulse, where the amplitude transfers between electronic states is the highest, the system still lies in a separable state. This is because the wave packets did not have any time to move and are still all localized in the Franck-Condon region of the molecule. As soon as the wave packets begin to move on their respective potential energy surfaces, the entanglement of the state increases. Similarly, the appearance of new singular values in the description of the state of the system is correlated with the differing motions of wave packets on different potential energy surfaces.

In addition to the differing gradients of the electronic states, non-adiabatic couplings (NAC) also play a role in the evolution of the entanglement

of the system. Their role can be highlighted by comparing the previous computational simulation with a simulation excluding the impact of NACs. A comparison of the evolution through time of the singular values for both the original computation and the one without NACs is shown in figure 7. This figure provides further insight in the time-evolution of the third and fourth singular values, as the moment of the onset of their rise changes strongly between the two simulations. It suggests that the effect of NACs on the entanglement of the state of the molecule is the strongest between 15 and 25 fs, and after that the main effect comes from the aforementioned difference in the gradients of the potential energy surfaces of each electronic state.

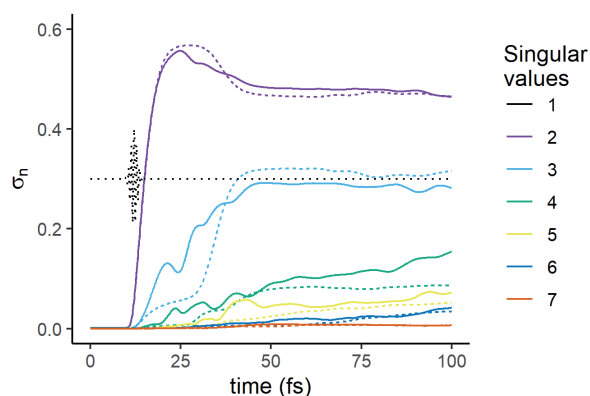


Figure 7: Evolution through time of the singular values for a simulation with non-adiabatic couplings (full lines) and without (dashed lines). The exciting optical pulse is represented in black. Reproduced from Ref. [25] with permission from the PCCP Owner Societies.

One way to verify this conclusion on the importance of the gradients of the electronic states is to study the singular vectors, which constitute an orthonormal basis for the states of the system, respectively for the nuclear degrees of freedom in the case of the left singular vectors and the electronic degrees of freedom for the right singular vectors. The singular vectors corresponding to the first four states of the SVD are shown in figure 8 and figure 9.

These two figures show the left singular vectors associated with each singular value, which represent a nuclear state and thus a localization on the grid, and the right singular vectors displaying an electronic state and thus a sort of “electronic composition” of the state in the SVD considered.

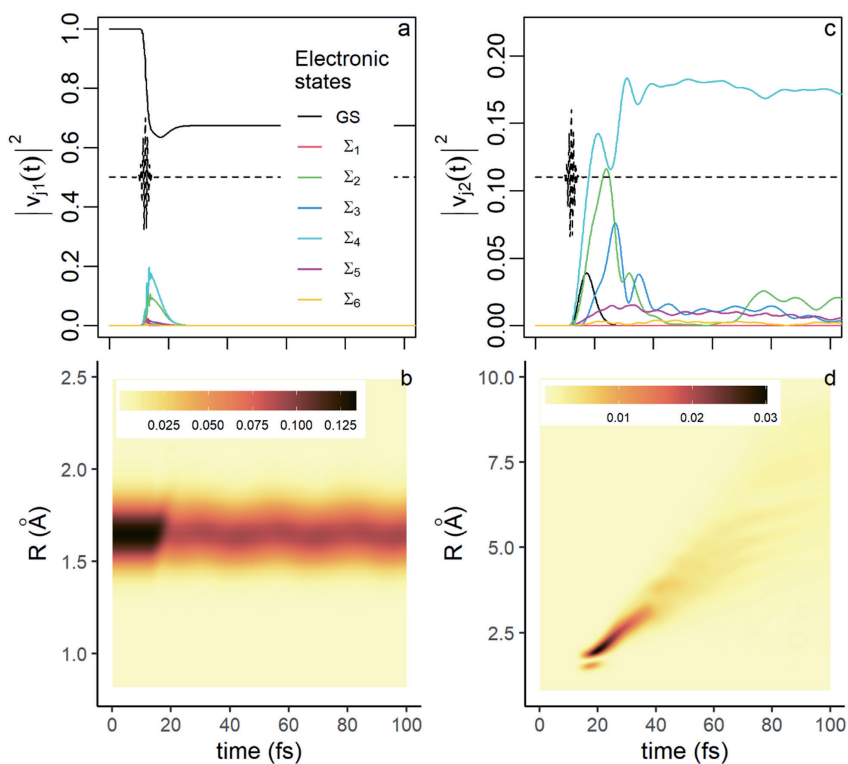


Figure 8: Left and right singular vectors associated with the first and second singular values. They are weighted by the singular values in order to better describe their importance for the description of the state of the system. Reproduced from Ref. [25] with permission from the PCCP Owner Societies.

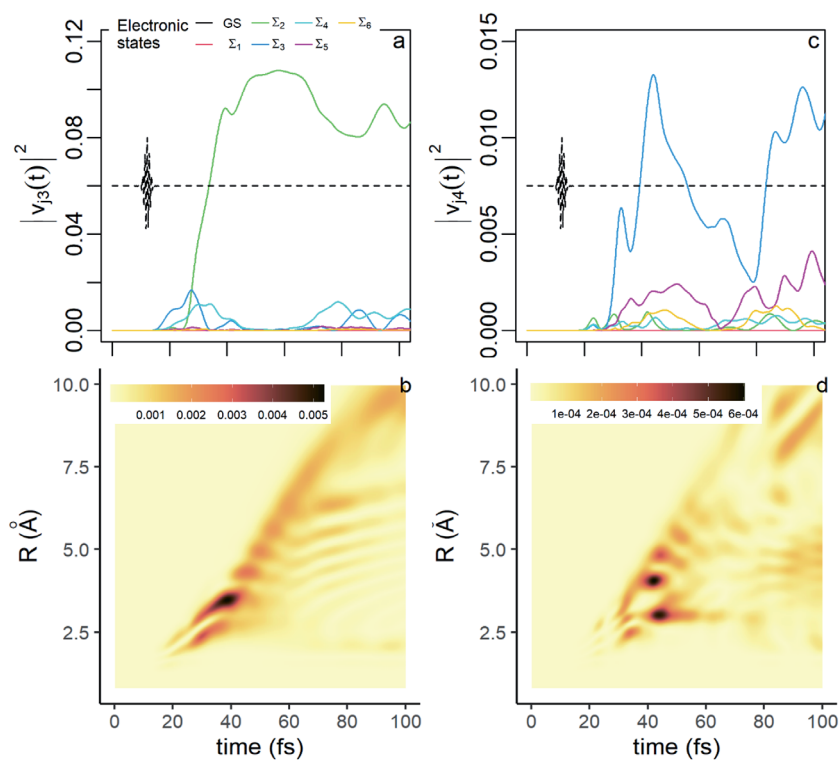


Figure 9: Left and right singular vectors associated with the third and fourth singular values. They are weighted by the singular values in order to better describe their importance for the description of the state of the system. Reproduced from Ref. [25] with permission from the PCCP Owner Societies.

This information confirms and improves the previous analysis that was performed on the basis of the singular values alone. The figures 8a and 8b show that the state associated with the first singular value is mostly composed of the ground state of the molecule and localized in the Franck-Condon region, except during the interaction with the optical pulse where a part of this state is localized on the excited electronic states, reflecting the previous note on the increase of the second singular value after the peak of the exciting pulse.

The subsequent singular vectors allow us to understand the appearance of the third singular value. The electronic composition of the second singular state (figure 8c) shows that it corresponds initially (just after the pulse) to a state with contributions of both the Σ_4 and Σ_2 ; electronic states, but then quickly loses its Σ_2 component as the wave packets of these two electronic states exhibit different motions on their respective potential energy surfaces. This timing is consistent with the rise of the third singular value, mainly localized on the Σ_2 electronic state (see figure 9a). The left singular vectors indicate that the wave packets corresponding to the second, third and fourth singular values all display a dissociative behaviour, their trajectory escaping from the Franck-Condon region of the system.

This constitutes a short overview of how SVD allows for some insight into the evolution of the entanglement in the simple molecular system which is LiH. Further information can be found in the article Blavier et al. [25].

4. Conclusion

The complex phenomena and behaviours arising from the interaction of matter with ultrafast optical pulses is at the same time one of the strongest motivations for the study of attosecond chemistry, and also the main reason for which such research is far from being straightforward. The purely coherent quantum dynamics created by the significant energy bandwidth of the attopulses used force us to perform fully quantum

dynamics on molecular systems, which remains for the moment a computationally intensive endeavour. Those issues constitute a significant bottleneck for the in-depth study of experimental data and the rationalization of the interactions between ultrashort pulses and molecules, which could enable a first step towards preparative or synthetic attochemistry.

These technical considerations aside, the study of attochemistry is also hampered, both experimentally and theoretically, by the amount and the complexity of the data produced which tremendously complicates their analysis, leading to another restraint in our ability to more finely understand attochemical phenomena.

Therefore, any technique which might accelerate or simplify either theoretical computations or data analysis and could improve our understanding of the coherent effects at play is important. As discussed in this article, singular value decomposition seems to be a valuable candidate for both considerations. It allowed us to reduce tremendously the number of initial states to consider to describe the random orientations of the molecules in the dynamics of the ultrafast Jahn-Teller rearrangement of the methane cation, leading to a significant decrease in the computational work required to model the evolution of the system, while keeping a good agreement with experimental results. Used as a method to compute the Schmidt decomposition of the wavefunction in LiH, it allowed a characterization of the time-evolution of the entanglement of the state of the system, providing novel insight in the interplay of nuclear and electronic degrees of freedom in molecular quantum dynamics.

It is almost certain that the singular value decomposition and similar algebraic decomposition will continue to find new uses in the analysis of ultrafast coherent molecular dynamics, as their handiness has now evaded the field of the statistics and linear algebra to enable new insights and provide solutions to problems in other fields.

Acknowledgements

This work was supported by the Fonds National de la Recherche Scientifique (Belgium), F.R.S.-FNRS research grants # T.0205.20. Computational resources have been provided by the Consortium des Equipements de Calcul Intensif (CECI), funded by the F.R.S.- FNRS under Grant # 2.5020.11. Support of the COST action Attochem (CA18222) is acknowledged. Support of the FRIA is also acknowledged.

The author would like to greatly thank Pr. Françoise Remacle, without whom all this work would not have been possible. Her review on the present manuscript proved to be instrumental to its quality. The author would also like to thank Kyde Bellon for his kind proofreading of this manuscript.

References

- [1] Balzani, V. Photochemistry and Photophysics: Concepts, Research, Applications. **2014**, 502.
- [2] Corkum, P. B.; Krausz, F. Attosecond Science. *Nat. Phys.* **2007**, *3* (6), 381–387.
- [3] Remacle, F.; Levine, R. D. An Electronic Time Scale in Chemistry. *Proc. Natl. Acad. Sci.* **2006**, *103* (18), 6793–6798.
- [4] Kling, M. F.; Vrakking, M. J. J. Attosecond Electron Dynamics. *Annu. Rev. Phys. Chem.* **2008**, *59* (1), 463–492.
- [5] F. Lépine, M. Y. Ivanov, M. J. Vrakking, J. Nat. Photonics 2014, *8* (3), 195–204.
- [6] Nisoli, M.; Decleva, P.; Calegari, F.; Palacios, A.; Martín, F. Attosecond Electron Dynamics in Molecules. *Chem. Rev.* **2017**, *117* (16), 10760–10825.
- [7] Zewail, A. H. Femtochemistry: Atomic-Scale Dynamics of the Chemical Bond. *J. Phys. Chem. A* **2000**, *104* (24), 5660–5694.
- [8] Reiter, S.; Keefer, D.; Vivie-Riedle, R. Exact Quantum Dynamics (Wave Packets) in Reduced Dimensionality. In *Quantum Chemistry and Dynamics of Excited States*; González, L., Lindh, R., Eds.; Wiley, 2020; pp 355–381.
- [9] Cohen-Tannoudji, C.; Diu, B.; Laloë, F. *Mécanique Quantique*; Collection Enseignement des sciences, 16; Hermann: Paris, 1973.
- [10] Levine, I. N. *Quantum Chemistry*, Seventh edition.; Pearson: Boston, 2014.
- [11] C. E. M. Gonçalves, R. D. Levine, F. Remacle, Phys. Chem. Chem. Phys. 2021, *10.1039/D1CP01029H*.
- [12] Ajay, J. S.; Komarova, K. G.; Van Den Wildenberg, S.; Remacle, F.; Levine, R. D. CHAPTER 9. Attophotochemistry: Coherent Electronic Dynamics and Nuclear Motion. In *Theoretical and Computational Chemistry Series*; Vrakking, M. J. J., Lépine, F., Eds.; Royal Society of Chemistry: Cambridge, 2018; pp 308–347.
- [13] Born, M.; Oppenheimer, R. Zur Quantentheorie der Molekeln. *Ann. Phys.* **1927**, *389* (20), 457–484.
- [14] Matsika, S. Electronic Structure Methods for the Description of Nonadiabatic Effects and Conical Intersections. *Chem. Rev.* **2021**, *121* (15), 9407–9449.
- [15] van den Wildenberg, S.; Mignolet, B.; Levine, R. D.; Remacle, F. Temporal and Spatially Resolved Imaging of the Correlated Nuclear-Electronic Dynamics and of the Ionized Photoelectron in a Coherently Electronically Highly Excited Vibrating LiH Molecule. *J. Chem. Phys.* **2019**, *151* (13), 134310.
- [16] Shiner, A. D.; Schmidt, B. E.; Trallero-Herrero, C.; Wörner, H. J.; Patchkovskii, S.; Corkum, P. B.; Kieffer, J.-C.; Légaré, F.; Villeneuve, D. M. Probing Collective MultiElectron Dynamics in Xenon with High-Harmonic Spectroscopy. *Nat. Phys.* **2011**, *7* (6), 464–467.
- [17] Abdi, H.; Williams, L. J. Principal Component Analysis: Principal Component Analysis. Wiley Interdiscip. Rev. Comput. Stat. 2010, *2* (4), 433–459.
- [18] Andrews, H.; Patterson, C. Singular Value Decomposition (SVD) Image Coding. *IEEE Trans. Commun.* **1976**, *24* (4), 425–432.
- [19] Alter, O.; Brown, P. O.; Botstein, D. Singular Value Decomposition for Genome-Wide Expression Data Processing and Modeling. *Proc. Natl. Acad. Sci.* **2000**, *97* (18), 10101–10106.
- [20] Remacle, F.; Kravchenko-Balasha, N.; Levitzki, A.; Levine, R. D. Information-Theoretic Analysis of Phenotype Changes in Early Stages of Carcinogenesis. *Proc. Natl. Acad. Sci.* **2010**, *107* (22), 10324–10329.
- [21] H. Abdi, in ‘Encyclopedia of measurement and statistics’, Eds. N. J. Salkind, K. Rasmussen, Thousand Oaks, Calif, 2007, p. 14.
- [22] Marangos, J. P.; Baker, S.; Kajumba, N.; Robinson, J. S.; Tisch, J. W. G.; Torres, R. Dynamic Imaging of Molecules Using High Order Harmonic Generation. *Phys Chem Chem Phys* **2008**, *10* (1), 35–48.
- [23] M. Blavier, K. Komarova, C. E. Gonçalves, R. D. Levine, F. Remacle, J. Phys. Chem. A 2021, *125* (43), 9495–9507.
- [24] A. Ekert, P. L. Knight, Am. J. Phys. 1995, *63* (5), 415–423.
- [25] M. Blavier, R. D. Levine, F. Remacle, Phys. Chem. Chem. Phys. 2022, *24*, 17516–17525.
- [26] Nielsen, M. A.; Chuang, I. L. *Quantum Computation and Quantum Information*, 10th anniversary ed.; Cambridge University Press: Cambridge ; New York, 2010.
- [27] Horodecki, R.; Horodecki, P.; Horodecki, M.; Horodecki, K. Quantum Entanglement. *Rev. Mod. Phys.* **2009**, *81* (2), 865–942.
- [28] Zhao, S.-F.; Xu, J.; Jin, C.; Le, A.-T.; Lin, C. D. Effect of Orbital Symmetry on the Orientation Dependence of Strong Field Tunnelling Ionization of Nonlinear Polyatomic Molecules. *J. Phys. B At. Mol. Opt. Phys.* **2011**, *44* (3), 035601.
- [29] Lein, M. Attosecond Probing of Vibrational Dynamics with High-Harmonic Generation. *Phys. Rev. Lett.* **2005**, *94* (5), 053004.

Damien MAHAUT,^{1,2} Benoit CHAMPAGNE,² and Guillaume BERIONNI¹

¹ Laboratoire de Réactivité et Catalyse Organique (RCO),

² Laboratoire de Chimie Théorique (LCT)

Department of Chemistry, Namur Institute of Structured Matter (NISM)

University of Namur, Rue de Bruxelles 61, B-5000 Namur, Belgium



Frustrated Lewis pair chemistry: early concepts, scope, and recent developments with 9-phosphatriptycenes

This article is part of the PhD thesis of the author, under the supervision of Prof. G. Berionni (experimental part) and Prof. B. Champagne (computational part).

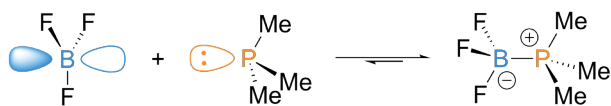
Abstract

Frustrated Lewis pairs (FLPs) chemistry provide new prospects in metal-free catalysis. Since their discovery in 2006 and the definition of the concept, these sterically hindered combinations of Lewis acids and bases have been increasingly used as catalysts for hydrogenation reactions. Over the years the scope of substrates expanded significantly, and mechanistic investigations shed light into their reactivity. Still challenges and limitations remain, and the hydrogenation of weakly reactive substrates such as “unactivated” olefins cannot be achieved by classical FLP systems. The groups of Prof. G. Berionni and Prof. B. Champagne at UNamur investigated the use of 9-phosphatriptycenes in this context. Due to their unique reactivity compared with other arylphosphines, these cage-shaped Lewis bases allowed for the first time the metal-free hydrogenation of unactivated olefins with FLP catalysts.

1. Frustrated Lewis pair chemistry

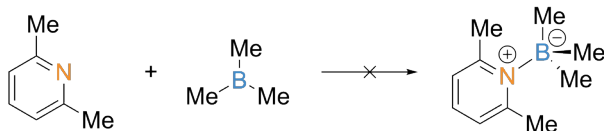
1.1. From the Lewis theory to the definition of frustrated Lewis pairs

The pioneer work of Gilbert Lewis on acids and bases in 1923 led to the development of one of the most important and unifying theories of reactivity in modern chemistry.¹ Lewis defined acids and bases as, respectively, electron-pair acceptors and donors. According to him, both react to form covalently bonded adducts, effecting a mutual stabilization (*i.e.* quenching) of the two compounds, as shown with the example of the association of trimethylphosphine with boron trifluoride (Scheme 1). Both compounds are unstable to air, but the Lewis adduct they form is stable in air and water. The concept of donor-acceptor adduct formation is ubiquitous in all aspects of chemistry, spanning from the coordination chemistry of transition metals, the rationalization of reaction mechanisms, the adsorption at the surface of materials in solid state chemistry or polymer science, up to the development of new catalysts.



Scheme 1. Reaction of a Lewis acid (boron trifluoride) and a Lewis base (trimethylphosphine), to form a Lewis adduct. The lone pair of electrons of the phosphorus atom overlaps the empty 2p orbital of the boron atom to form a covalent bond.

Frustrated Lewis pair chemistry provides new prospects in acid-base chemistry, where the reactivity of Lewis acids and bases are combined while preventing mutual quenching. This point is detailed below. According to the Lewis theory [1], a Lewis base (e.g. PR_3) combines with a Lewis acid (e.g. BX_3) to form a covalent adduct ($\text{R}_3\text{P}\rightarrow\text{BX}_3$). However, the subtle effect of steric hindrance on their association was investigated later. In their 1942 report, Brown and coworkers studied the effect of steric strain on carbon-carbon bond rotation by comparing the stability of a series of amine-borane adducts (the B-N bond being isosteric to the C-C bond). They observed that the 2,6-lutidine does not coordinate with trimethylborane due to the excessive steric strain the B-N bond formation would generate (Scheme 2) [2].

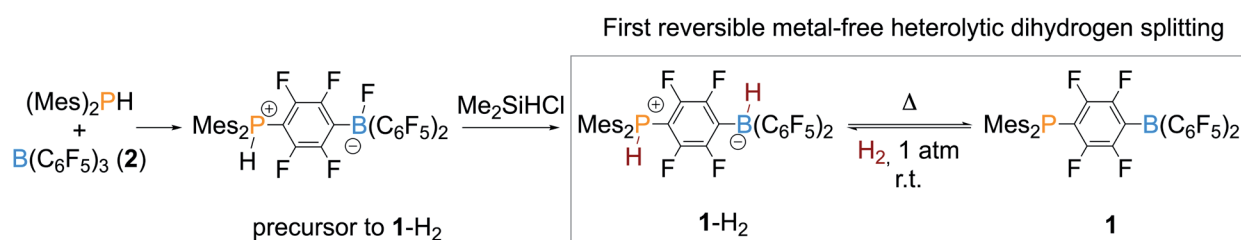


Scheme 2. Absence of reaction between 2,6-lutidine and trimethylborane.

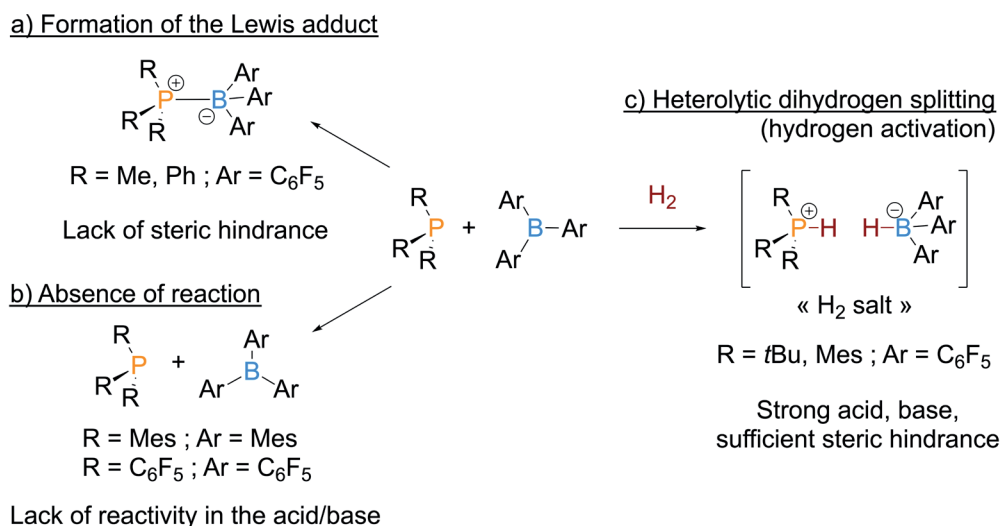
In 2006, Stephan discovered that a phosphine-borane compound (**1**) was able to reversibly react with and release dihydrogen (H_2) [3]. The reaction

of **1** with H_2 is spontaneous at room temperature under 1 atm of dihydrogen while H_2 release is triggered by heating above 100°C (Scheme 3). Due to steric hindrance, dimesitylphosphine (Mes_2PH , $\text{Mes} = 2,4,6\text{-trimethylphenyl}$) and tris(pentafluorophenyl)borane **2** did not form the classical Lewis adduct but instead, under heating, generated the precursor to **1** via nucleophilic aromatic substitution at the *para* position of a C_6F_5 ring of **2**, leading to this seminal discovery. It constituted the first reported reversible metal-free hydrogen activation. While other phosphine-borane systems are capable of releasing H_2 , the unique stability of **1** (i.e. the lack of polymerization or cyclization) is due to the steric hindrance around the P and B centers and allows its reversible reaction with H_2 .

In his subsequent report, Stephan investigated the steric and electronic parameters influencing this reactivity [4]. More classical and simple frustrated pairs than **1** were shown to cleave dihydrogen, such as the $\text{PtBu}_3/\text{B}(\text{C}_6\text{F}_5)_3$ or $\text{PMe}_3/\text{B}(\text{C}_6\text{F}_5)_3$ combinations. Not all phosphine/borane pairs are suitable however, as the steric hindrance in the acid or the base must be sufficient to prevent the formation of the Lewis adduct, while their acidity/basicity must remain high enough for reacting with dihydrogen. On the one hand, the combinations PMe_3 or $\text{PPh}_3/\text{B}(\text{C}_6\text{F}_5)_3$ for instance are lacking in steric repulsions and form a classical Lewis adduct. On the other hand, $\text{PMes}_3/\text{BMes}_3$ or $\text{P}(\text{C}_6\text{F}_5)_3/\text{B}(\text{C}_6\text{F}_5)_3$ do not react spontaneously with H_2 at room temperature because they are electronically deactivated, either the acid or the base is not reactive enough to cleave dihydrogen (Scheme 4) [4].



Scheme 3. First example of reversible heterolytic hydrogen splitting reported by Stephan.

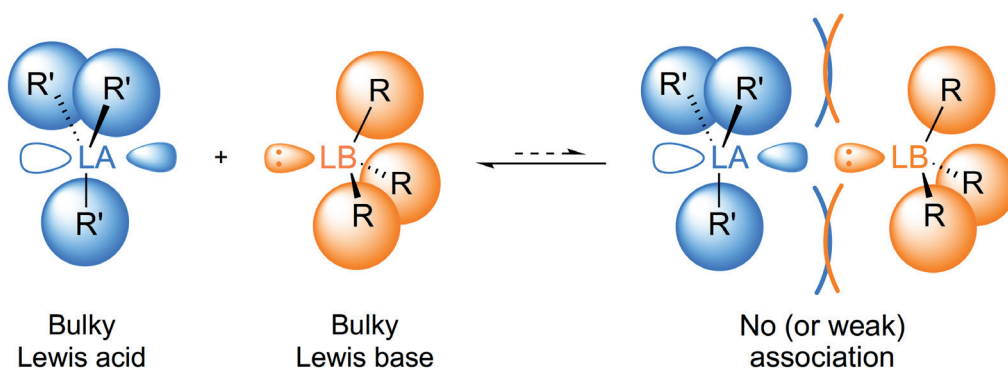


Scheme 4. Reactions of Lewis acid-base combinations in the presence of dihydrogen according to their substitution pattern.

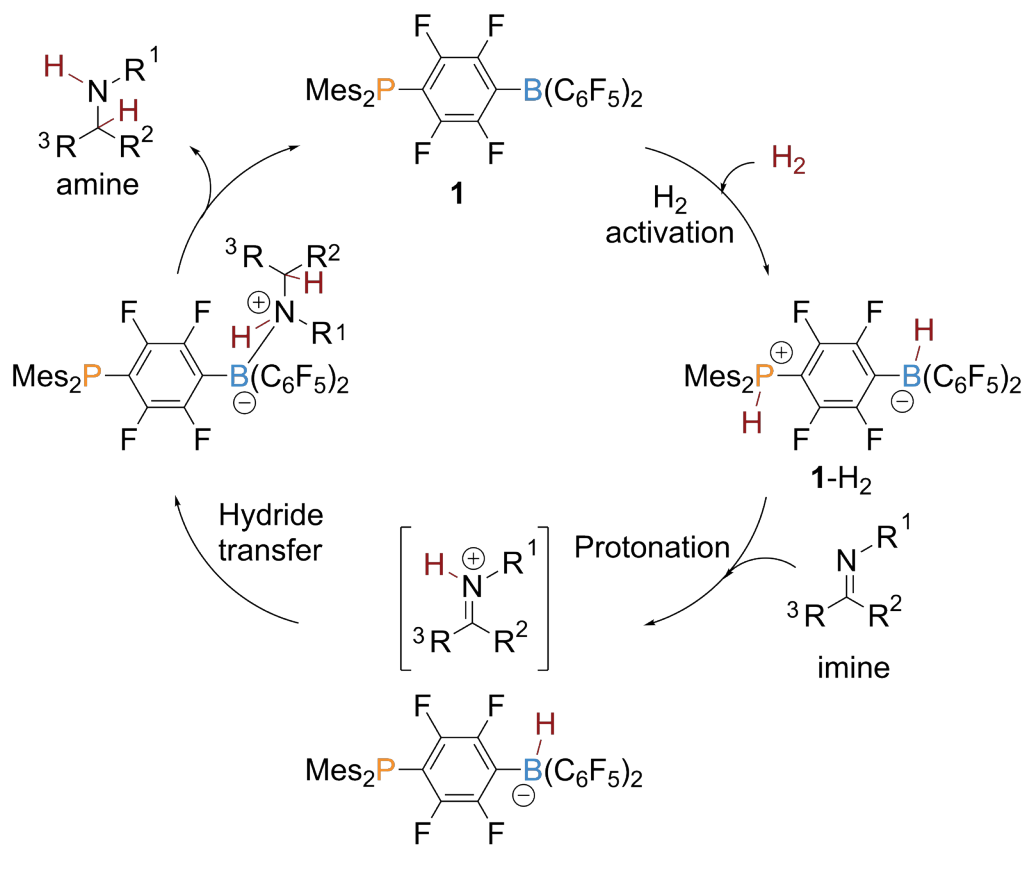
These observations eventually led to the formal definition of “frustrated Lewis pairs” (FLPs) as sterically hindered Lewis acids and bases that cannot form the corresponding Lewis adduct because of steric repulsions (Scheme 5) [5-6]. These bifunctional systems display completely new reactivity patterns and even some catalytic properties since both Lewis acid and base are now able to act synergistically on a reagent of small size in a “three-component” type reaction.

Stephan next demonstrated the ability of these systems to perform the metal-free hydrogenation of unsaturated substrates, namely imines and

nitriles, and the reductive ring-opening of aziridines with dihydrogen [7]. The hydrogenation reaction was proposed to proceed as follows: first, the heterolytic splitting of H₂, generating formally a proton (phosphonium) at the Lewis base and an hydride (borohydride) at the Lewis acid, followed by proton transfer to the imine then hydride transfer to the iminium moiety, forming a new B-N bond, finally followed by the release of the corresponding amine and regeneration of the catalyst (Scheme 6). Hydrogenations with FLP systems was an important part of my PhD work, and a more detailed subsection on this reactivity is detailed hereafter.



Scheme 5. Stephan's definition of a frustrated Lewis pair.



Scheme 6. Proposed mechanism for an imine hydrogenation by FLP system **1**. Scheme adapted from reference [8] with permission from the Royal Society of Chemistry.

1.2. Reactivity of frustrated Lewis pairs

1.2.1. First hydrogenations and hydrogenation of alkenes and alkynes

Hydrogenation reactions are among the most widely used chemical transformations, especially in pharmacochemical industries and synthetic organic chemistry [9-10]. Ever since the founding work of Sabatier in the beginning of the 20th century, homogeneous and heterogeneous transition-metal-based catalysts were used for these transformations [11-13]. However, the limited resources and toxicity of these elements incite chemists to develop alternatives [14-17]. As shown above, frustrated Lewis pairs are able to catalyze the hydrogenation of unsaturated substrates and thus constitute appealing surrogates to transition metal catalysts for this transformation. While other transition-metal-free systems are known to catalyze hydrogenations, they either require harsh

conditions or use other sources of hydrogen, such as Hantzsch's ester (in hydride transfer reactions) or hydrogen transfer reagent surrogates [18-25]. FLPs offer the advantage of reacting directly with H₂. In addition, the reactivity of the Lewis acid and base can be finely tuned to target different types of substrates. Over the years, these systems were extensively used for transition-metal-free hydrogenations of unsaturated compounds, notably imines, alkenes, aromatics, and carbonyl compounds. Several comprehensive publications have reviewed these hydrogenation reactions, their scope and limitations [8, 26-28].

As mentioned above, the first report of FLP-catalyzed hydrogenation described the transformation of imines, nitriles and aziridines to the corresponding amine. The phosphonium hydridoborate salt of **1** and another *t*Bu-substituted derivative were used as catalysts [7]. The reaction yields were dependent on the steric and electronic

the group of Paradies in collaboration with Stephan reported the first hydrogenation of olefins [36]. For this transformation, they used deactivated Lewis bases such as $\text{P}(\text{C}_6\text{F}_5)(\text{Ph})_2$ (Scheme 7a). Upon hydrogen activation, these weaker bases generate a phosphonium cation with enhanced Brønsted acidity, able to protonate a carbon-carbon double bond. The carbenium ion formed after protonation is stabilized by conjugation with either aryl substituents or neighboring unsaturated bonds in the substrate. The borohydride then adds on the carbocation to yield the alkane as product. These FLP systems appear not to react spontaneously with dihydrogen at room temperature, and low temperatures (between -60°C and -80°C) are needed to observe the phosphonium and borohydride by NMR spectroscopy. However, it does not prevent the hydrogenation to proceed at room temperature, and olefins are reduced in reaction times between 12 h and 96 h, with longer times and higher temperatures required for less reactive double bonds (up to 240h and 70°C). Interestingly, Stephan showed that dialkylethers/ $\text{B}(\text{C}_6\text{F}_5)_3$ combinations can catalyze 1,1-diphenylethylene hydrogenation, although requiring higher pressures of H_2 to proceed [37]. Similarly, polycyclic aromatic cycles and N-heteroaromatics are partially reduced with these FLP catalysts [38-41].

In contrast to this reactivity, Alcarazo showed that olefins can also act as hydride acceptors if the resulting carbanion is stabilized by electron-withdrawing groups (Scheme 7b). In this case, the hydride transfer happens first and is followed by the protonation step [42-44].

While not technically an FLP catalyst, Wang's hydrogenation of aliphatic olefins catalyzed by Piers' borane [bis(pentafluorophenyl)borane, $\text{HB}(\text{C}_6\text{F}_5)_2$] is worth mentioning (Scheme 7c) [45]. These less reactive alkenes are not readily hydrogenated by standard FLP systems. Their formal hydrogenation is achieved by initial hydroboration of the alkene by the borane, followed by σ -bond metathesis with H_2 , or hydrogenolysis, of the carbon-boron bond (Scheme 7d). The metal-free catalytic hydrogenation of olefins was already known in the literature (Scheme 7e), dating back to the

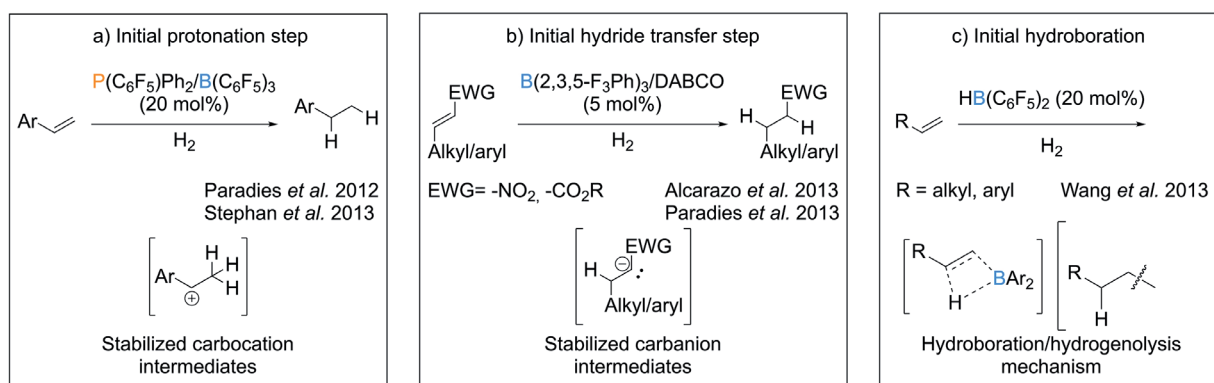
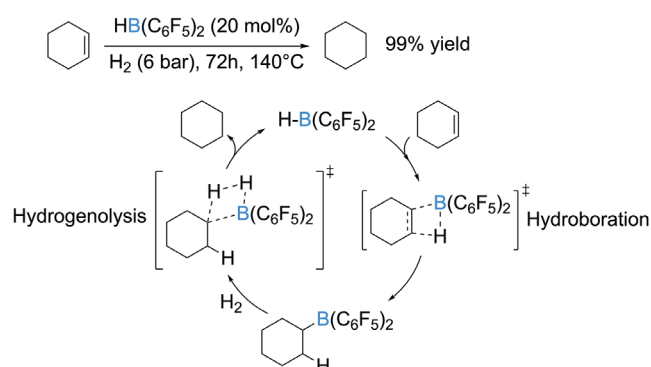
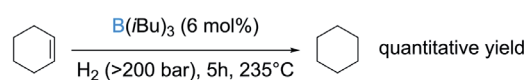
1960's [46-47], but the reaction of Wang *et al.*, performed at 140°C under 6 bar of hydrogen pressure and 20 mol% catalyst, constitutes the first reported example of metal-free-catalyzed hydrogenation of aliphatic, unactivated alkenes, under relatively mild conditions. They took advantage of the better reactivity of Piers' borane for hydroborations compared to classical boranes to perform this challenging reaction [48].

The first step toward the hydrogenation of alkynes was reported by the group of Erker. Their intramolecular FLP **3** reduced ynones into the corresponding enones [49]. The hydrogenation of simple alkynes however was reported later by Repo and coworkers [50]. Using an *ansa*-aminoborane system **6**, they performed the hydrogenation of alkynes to *cis*-alkenes under mild conditions (Scheme 8). The actual catalyst **6** is generated by reacting the pre-catalyst **5** at 80°C under H_2 atmosphere. The new B-H bond allows the following hydroboration of the substrate, generating a bulky bifunctional system **7** which cleaves H_2 to form the corresponding ammonium hydridoborate salt **7-H₂**, eventually releasing the *cis*-alkene *via* protodeborylation. Hydrogenation with this system only yields the *cis*-alkene (*Z*). Subsequent work by Du described the selective hydrogenation to *cis*- or *trans*-alkenes catalyzed by $\text{HB}(\text{C}_6\text{F}_5)_2$, in a similar fashion as Wang for unactivated alkenes [51].

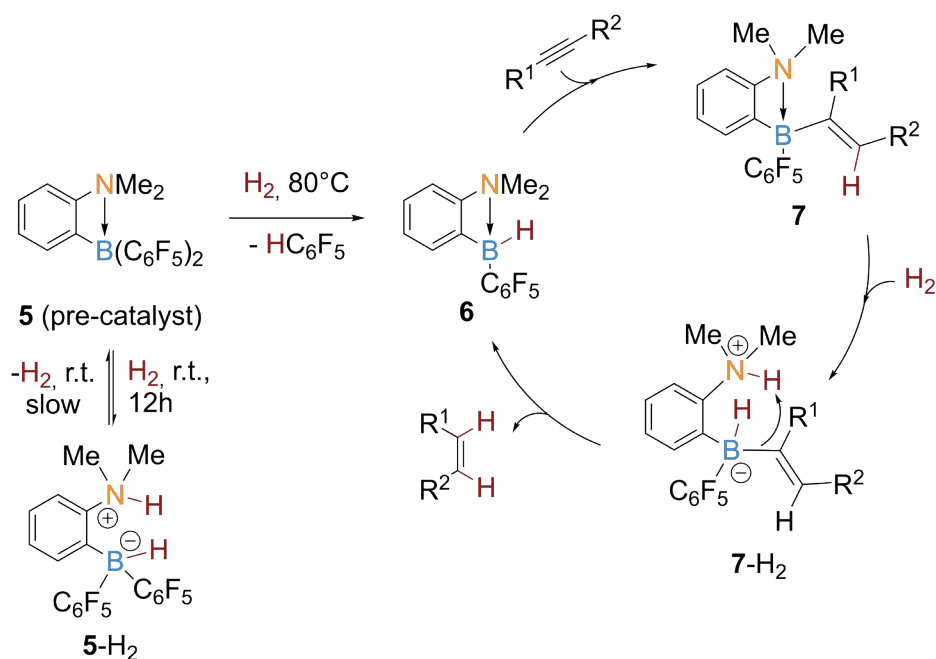
1.2.2. Hydrogenation of carbonyl derivatives

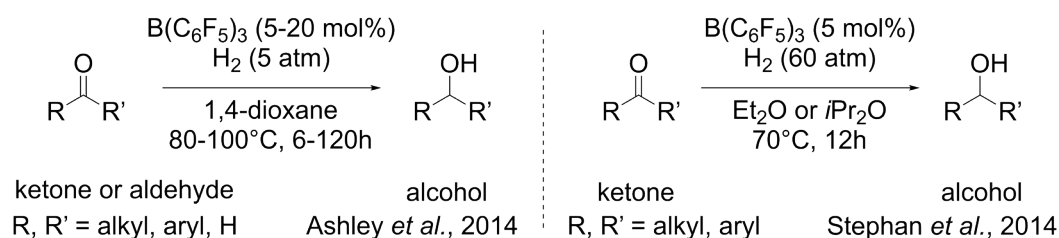
The use of ethereal solvents developed by Stephan and Ashley allowed the hydrogenation of aldehydes and ketones. These substrates turned out to be more challenging than their imines analogues due to the lower basicity of the oxygen atom. By computational investigation, Privalov reported that the process of activating H_2 with a ketone in combination with $\text{B}(\text{C}_6\text{F}_5)_3$ was possible [52]. Early efforts however were unsuccessful and only led to the formation of the corresponding alkoxyboranes and the deactivation of the catalyst [53-54]. Eventually, the groups of Ashley and Stephan solved this problem by using respectively THF or diethyl ether/diisopropyl ether as solvents (Scheme 9) [55-56].

Three pathways of olefins hydrogenation

d) (Wang *et al.* 2013) Mechanism: Example of cyclohexenee) (Trapasso *et al.* 1961) First example by hydroborationHydridoborane generated *in situ* in the presence of H₂

Scheme 7. Metal-free-catalyzed hydrogenations of olefins, either by FLPs or Piers' borane. DABCO = 1,4-diazabicyclo[2.2.2]octane.

Scheme 8. Formation of the catalyst **6** and mechanism of FLP-catalyzed hydrogenation of alkynes to cis-alkenes.



Scheme 9. FLP-catalyzed hydrogenation of ketones and aldehydes by Ashley and Stephan.

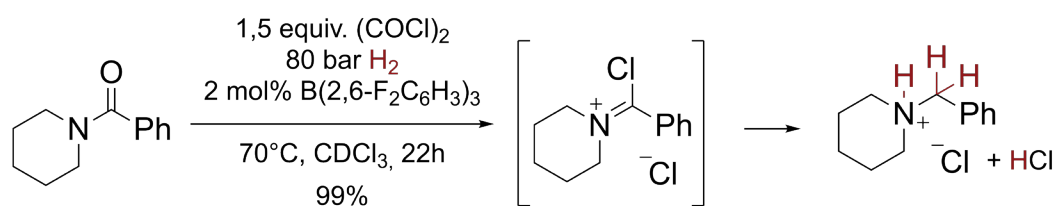
Investigating the reactivity of the Lewis acid also expanded the scope of FLP chemistry. Soós *et al.* reported the use of bulkier and weaker Lewis acids for the hydrogenation of Michael acceptors, previously limited by their coordination to the oxygen atom, and carbonyl compounds [32, 35, 57]. The first water-tolerant FLPs were developed this way, allowing the catalysis of a new reaction by FLPs, reductive aminations, not considered earlier since it generates water as by-product [58-59].

The reduction of amides is one of the major ways to form functionalized amines [60]. The use of transition metal catalysts is well-developed but poses issues of selectivity (formation of a mixture of the corresponding amine and alcohol) and of tolerance with sensitive functional groups (*e.g.* halogens, alkynes, nitro). Paradies reported the first hydrogenation of amides by FLPs [61]. This reaction required $(\text{COCl})_2$ as additive to convert the amide in the corresponding chloroiminium ion before reduction to the ammonium (Scheme 10) [62]. Later improvements using a phosphine oxide in combination with triphosgene $[\text{CO}(\text{OCCl}_2)_2]$ to generate the chloroiminium intermediate were reported [63]. Similarly, esters eluded

FLP hydrogenation until recently, when Ashley reported their direct hydrogenation catalyzed by an organotin Lewis acid in combination with lutidine [64].

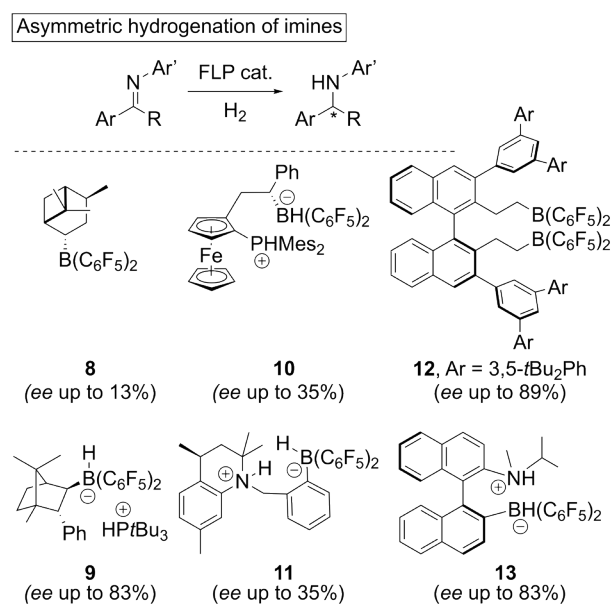
1.2.3. Enantioselective hydrogenations catalyzed by FLPs

In 2008, Klankermayer and his group opened the door of asymmetric catalysis with FLP catalysts when they used an alkenylborane derived from (+)- α -pinene (**8**, Scheme 11) to catalyze the enantioselective hydrogenation of imines [30]. This first chiral catalyst only led to limited enantiomeric excess (13% *ee*) but later improvements using a camphor scaffold (**9**, Scheme 11) led to *ee* values up to 83% for the same reaction [65-66]. Other chiral FLP systems were developed as well: Erker *et al.* used a ferrocene-based catalyst (**10**, Scheme 11) for asymmetric imine reduction with up to 69% *ee* [67-68]. Building on earlier work with intramolecular FLPs [33], Repo and coworker synthesized a series of *ansa*-ammonium borates systems including some chiral versions (**11**, Scheme 11) able to yield up to 35% *ee* [69]. Notably, the group of Du reported



Scheme 10. Paradies' hydrogenation of amide through a chloroiminium intermediate.

a straightforward method to access chiral Lewis acid catalysts based on the binaphthyl chiral scaffold [70]. Their catalyst **12** (Scheme 11) is generated in situ by double hydroboration of binaphthyl diene with Piers' borane [$\text{HB}(\text{C}_6\text{F}_5)_2$] and displays good enantioselectivity with up to 89% *ee*. Another well-performing system for asymmetric imine hydrogenation based on the naphthyl scaffold (**13**, Scheme 11) was reported by Repo. These bifunctional "chiral molecular tweezers" led to *ee* values up to 83% for imines and up to 99% for enamines [71].



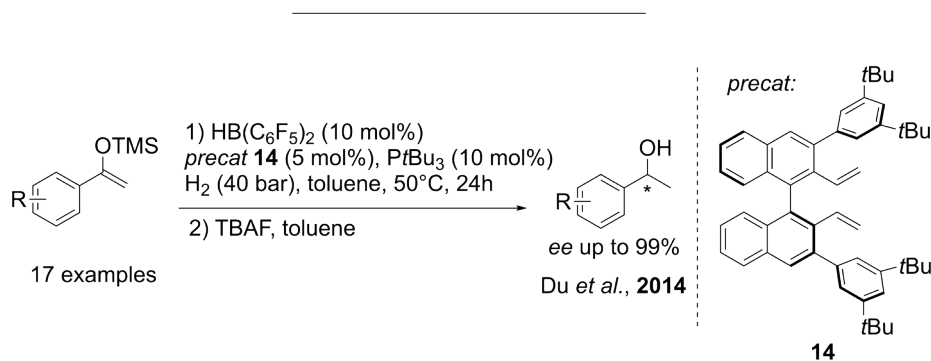
Scheme 11. General reaction of asymmetric hydrogenation of imines and selected examples of chiral FLP systems.

Other substrates were targeted as well, for example variations of Du's catalyst allowed the

hydrogenation of silyl enol ethers (**14**, Scheme 12) and N-heterocycles with good enantioselectivity [72-76].

1.2.4. Investigations on the mechanism of H_2 activation

Understanding the reactivity of frustrated Lewis pairs and the mechanism of hydrogen activation remains a challenge. To this end, many research groups have undertaken computational studies, mostly employing Density Functional Theory, to gain insight into the complex reactivity of FLPs [77-84]. In particular, the mechanism of H_2 activation by acid-base combinations was a source of long-lasting debates. Shortly after the seminal discoveries of Stephan, in 2008, Pápai and co-workers reported a quantum chemical study of the activation of dihydrogen by the typical FLP tris(*tert*-butyl) phosphine (Pt-Bu_3) and tris(pentafluorophenyl) borane ($\text{B}(\text{C}_6\text{F}_5)_3$) [77]. They pointed out that the splitting of the hydrogen molecule is neither due to a preliminary borane- H_2 or phosphine- H_2 complexation but to a concerted mechanism: a simultaneous breaking of the H-H bond and formations of P-H and B-H covalent bonds. The preliminary borane- H_2 complex was initially hypothesized because $\text{H}_3\text{B} \leftarrow \text{H}_2$ interactions were previously observed experimentally [85-86]. In the case of $\text{B}(\text{C}_6\text{F}_5)_3$ however, the weak electron-donation from the π -system to the vacant boron orbital is sufficient to prevent this interaction, due to Pauli repulsions. Instead, they suggested that the Lewis acid and the Lewis base associate first through weak interactions, without direct P-B

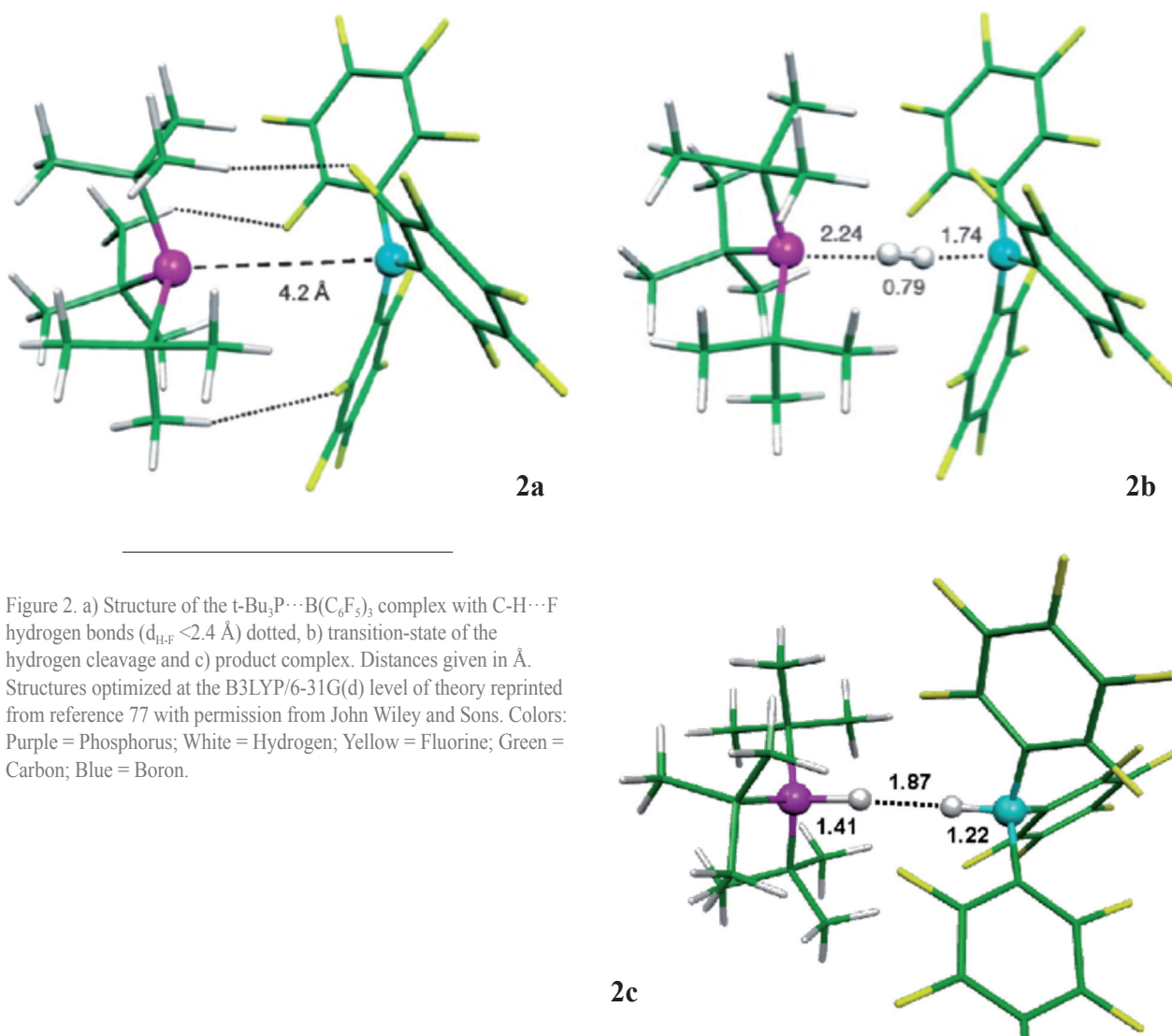


Scheme 12. Asymmetric hydrogenation of silyl enol ethers and deprotection to the secondary alcohol by Du *et al.* TBAF= tetrabutylammonium fluoride, TMS = trimethylsilyl.

charge transfer (mainly dispersion interactions and C-H \cdots F hydrogen bonds), to form a cavity in which H₂ can be inserted (Figure 2). The H-H bond heterolytic cleavage happens subsequently through a transition state stabilized by the same weak intermolecular interactions between the phosphine and the borane to form the product, itself further stabilized by a P-H \cdots H-B electrostatic interaction.

Their mechanism was later detailed based on a molecular orbital approach [87]. The LA-LB complex retains the HOMO of the base and the LUMO of the acid mostly unchanged but aligned in a way to ease orbital overlaps with H₂. The latter molecule inserted in the cavity undergoes a significant polarization (symmetry breaking) that alters its orbital configuration (mixing between the HOMO and LUMO of H₂) resulting in a H₂ molecule

acting both as a better electron pair acceptor and electron pair donor than in the unperturbed system (Scheme 13, left). The actual heterolytic splitting happens next through a simultaneous $LP_P \rightarrow \sigma_{H_2}^*$ and $\sigma_{H_2} \rightarrow p_B^*$ electron transfer, resulting in the phosphonium and borohydride ion pair. H₂ acts as a bridge between the acid and base centers, breaking its σ bond to release the frustration. Interestingly, they drew a parallel between this reactivity and the other modes of H₂ splitting, homolytic or heterolytic, in metal complexes or by singlet carbenes, identifying FLP-H₂ activation as the newest member in this category (Scheme 13, right). In view of all these results and the stabilization occurring in the product of the reaction, they could explain why, experimentally, this reaction happened quantitatively and under mild conditions.

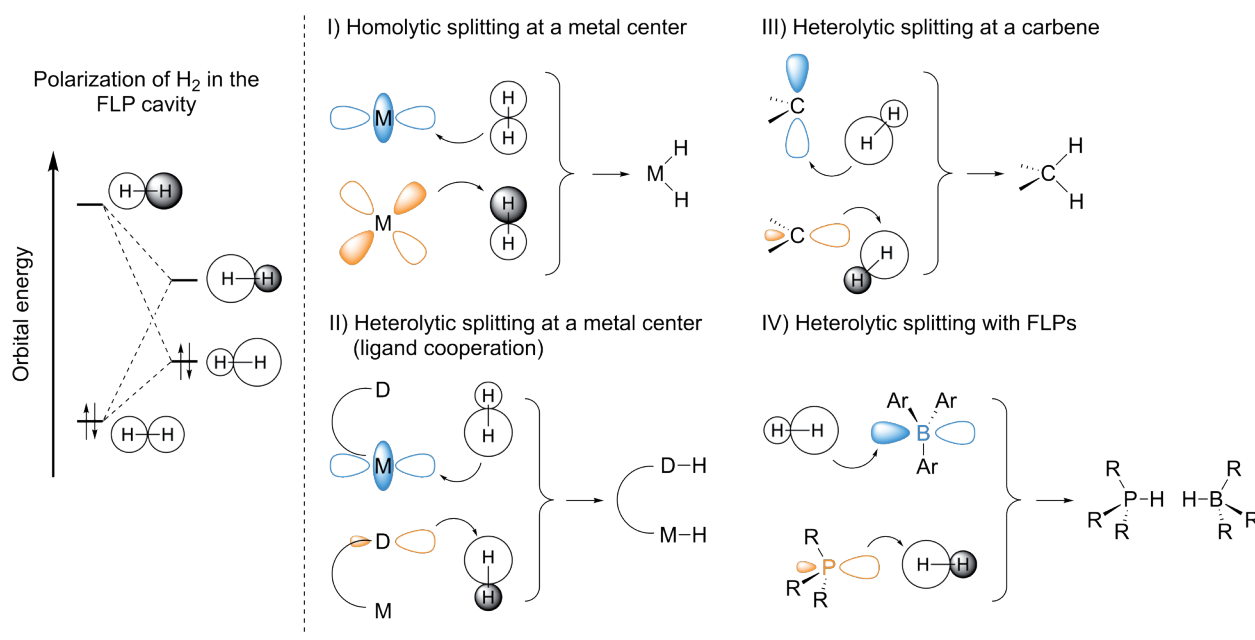


Similarly, Guo and Li invoked the same mechanism to explain the splitting of H_2 by Stephan's first intramolecular FLP system **1** [88], contrary to the mechanism proposed in that initial report [3].

Next were investigated the factors influencing the thermodynamics of H_2 activation by several acid-base combinations [78]. To this end, a partitioning of reaction energies was undertaken, identifying several unfavorable and favorable contributions, the former consisting in the H_2 cleavage itself and the preparation energy of the Lewis pair (breaking of eventual dative LA-LB bonds or weak interactions to "make space" for H_2 insertion), the latter consisting in the stabilizations brought by proton attachment to the Lewis base, the hydride attachment to the acid and the coulombic interactions in the ion pair product. Isolating these contributions allowed to pinpoint the individual effects of the acid, of the base, and of the nature of the FLP itself (either intra- or intermolecular). A notable conclusion from the report was that intermolecular FLPs displayed a good correlation between the strength of the acid-

base combination and the ease of H_2 cleavage, while intramolecular FLPs benefited from a reduced entropy penalty, so that weaker intramolecular acid-base combinations were still able to activate H_2 . In a later report, Vankova *et al.* drew similar conclusions for reaction kinetics [82]. Both articles stress the importance of tuning the size and properties of the Lewis base and of the Lewis acid to best exploit the reactivity with H_2 .

In 2010, Grimme and Erker challenged the so-called "electron transfer" mechanism of Papař, described above [89]. Their initial claim was that the previous work of Papař was questionable, mainly due to a poor theoretical treatment (namely the small, poorly flexible, basis set, the use of the B3LYP functional, and the lack of proper benchmark study for the method) that did not (sufficiently) consider the interactions between the bulky substituents, mainly London dispersion forces, and led to inaccurate transition state structures. Using the B97-D [90]/TZVPP^[1] [91] method in



Scheme 13. (left) Orbital deformation resulting from mixing between HOMO and LUMO. (right) Modes of H_2 splitting in a metal complex (I, II), at a carbene (III) and by FLPs (IV). In orange and in blue are shown filled and empty orbitals respectively, filled orbital of H_2 shown in full white, empty in black and white. Heterolytic splitting modes involve a polarized H_2 moiety. Scheme adapted from reference 87 with permission from John Wiley and Sons.

1 TZVPP^{*} corresponding to Alrich's triple ζ valence basis set with either two sets of polarization functions for P, B and H (TZVPP) or one set for all other atoms (TZVP).

combination with single point calculations at the higher-level SCS-MP2 [92] /CBS [93-94], they probed the potential energy surface in the cavities (Figure 2a) created in FLP systems at several P-B and H-H distances and concluded that once H_2 was inside the cavity, its dissociation was practically barrierless. They attributed the observed kinetic barrier to the H_2 entrance into the cavity. According to their mechanism, the electric field generated between the acid and the base centers is sufficient to split the H_2 molecule, the phosphorus and boron then acting merely as the hydride acceptor and donor. To support this view, they simulated a strong electric field acting on H_2 , without FLP system, and showed that the heterolytic splitting was spontaneous (Figure 3). According to them, there is no need to invoke orientation and deformation of molecular orbitals to explain FLP reactivity.

To summarize both conceptual views, in the electron transfer mechanism, FLPs activate H_2 by adequate orbital overlaps, allowing electron transfer. The reaction barrier is due to the transition state of H_2 splitting. In the electric field mechanism, FLPs activate H_2 through its polarization owing to the electric field generated by the LA and LB moieties. The reaction barrier is due to preparation or entrance of H_2 in the cavity.

Investigations in the following years discussed the possibilities of both mechanisms. Camaioni *et al.* studied a series of small molecules combinations (NH_3/BX_3 , $X=H, F, Cl$) in their reaction with H_2 [95]. They optimized their structures using B3LYP-D/DZVP2 method and refined electronic energies at the G3(MP2)-B3LYP [96] and CCSD(T) levels of theory. Given the study was not experimental, they could decide to ignore the fact that the small molecules would normally form Lewis adducts and focused instead on the energy decomposition analysis of their reaction with H_2 . They concluded that favorable orbital overlaps were the main stabilizing factor in reaction energy. Electrostatic interactions, which include the interactions through the electric field generated by the FLP, were significant as well but could not alone be accountable for the reactivity of the system.

Rokob, Papaï and co-workers eventually addressed the previous comments of Grimme on the theoretical method. New in-depth studies, extensively comparing both conceptual views, were reported [81, 97]. Inter- and intramolecular FLPs with several types of Lewis acids and bases were considered, eventually supporting the electron-transfer mechanism, and highlighting the limitations of the electric field view. To

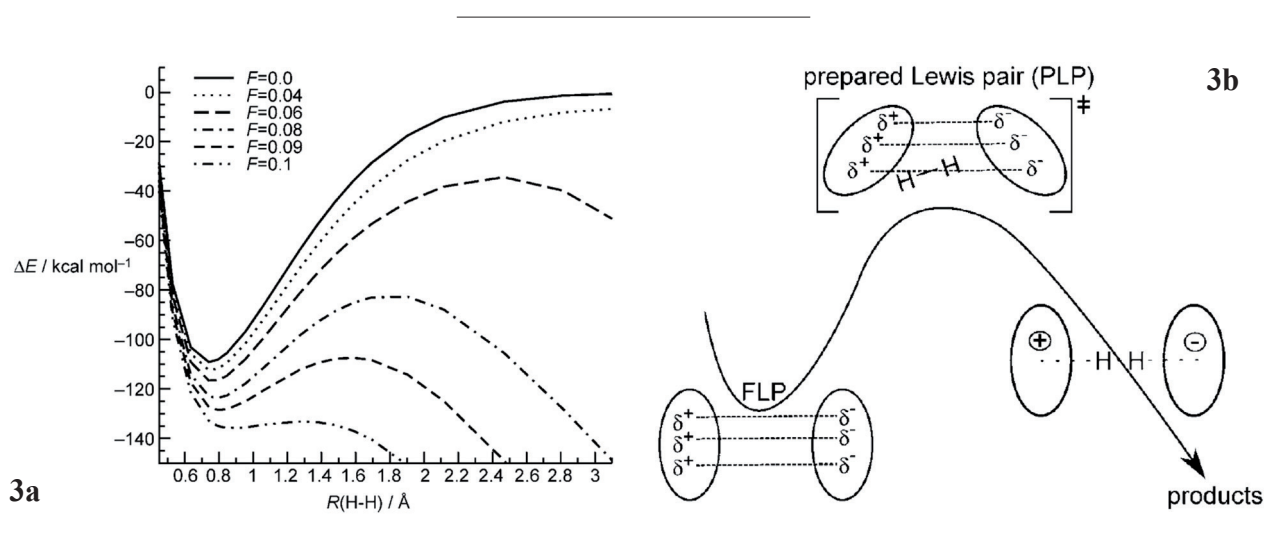


Figure 3. (left) Potential energy curves of H_2 dissociation (computed at the FCI/aug-cc-pVQZ) in electric fields of varying strength, note that for a strong enough field ≥ 0.1 a.u. ($1 \text{ a.u.} = 5.1422 \cdot 10^{11} \text{ V}\cdot\text{m}^{-1}$), the dissociation is almost barrierless. (right) Representation of FLP H_2 activation with the electric field model, a typical range of field strength inside a FLP is between 0.04 and 0.06 a.u. Schemes reprinted from reference [89] with permission from John Wiley and Sons.

further support their claim, they performed a preliminary benchmark study, investigating the effect of the method on the results and settled on the use of the ω B97X-D exchange correlation functional, a range-separated hybrid functional including an empirical dispersion correction term, with the 6-311G(d,f) basis set. Eventually, they proposed a general mechanism for intermolecular FLP systems, regardless of the nature of the LA and LB considered, divided in three main steps: i) preorganization through weak interactions, ii) simultaneous interaction of H_2 with both LA and LB (*i.e.* H_2 polarization) and iii) electron transfer through cooperative $LP_{LB} \rightarrow \sigma_{H_2}^*$ and $\sigma_{H_2} \rightarrow p_{LA}^*$. The mechanism differs between systems in the way H_2 , the electron donor and the acceptor are positioned.

These discussions pointed out the need for a robust computational method and how inappropriate exchange-correlation functionals or basis sets can lead to inaccurate structures, energies, or scientific conclusions. Even though the electron transfer model has been generally adopted overtime, especially since the molecular orbital approach allowed a deeper understanding and the establishment of guidelines for the development of new systems, continuous improvements and contributions were added over the years. The addition of Molecular Dynamics studies are worth mentioning, which allowed the group of Ensing to shed light on the asynchronous nature of the transition state and the individual roles of the acid and base on the kinetics [98-100]. Giving more depth to the established models, Privalov described more complex orbital interactions, in which both σ and σ^* orbitals of H_2 in the cavity are coupled with the HOMO and LUMO respectively of the

FLP system [101]. In essence, the understanding of reaction mechanisms and the interactions between all involved compounds through computational studies is crucial to predict the properties of FLPs and to design new ones.

1.2.5. Small molecules capture, carbon dioxide hydrogenation and methane activation

The reactivity of FLP systems is not limited to dihydrogen, several small molecules can be captured by FLPs, such as CO , CO_2 , SO_2 and N_2O (Figure 4) [102-108]. Reaction conditions are similar to the original H_2 reports [4]: the FLP spontaneously traps these small molecules at room temperature and atmospheric pressure of the gas. Contrary to H_2 however, no catalytic system has yet been developed with these molecules. They require a stoichiometric amount of phosphine-borane, which is why one talks of small molecules “capture” instead of “activation”.

The activation of CO_2 , a potent greenhouse gas [109], is a very attractive transformation, which led researchers to further investigate its reactivity with FLP catalysts. Its conversion with dihydrogen into formic acid or methanol is an attractive method to generate C_1 building blocks in chemical synthesis or as a chemical storage of H_2 in the context of renewable energy management [110-112]. This transformation is well-studied in heterogeneous catalysis [113-114], with electrochemical reduction [115] as well as with transition metal in homogeneous catalysis [116], but an efficient metal-free alternative is still lacking [117]. Wang reported a $B(C_6F_5)_3$ -catalyzed hydrogenation of carbon dioxide without transition metal but using instead potassium metal (K) in the reaction mixture

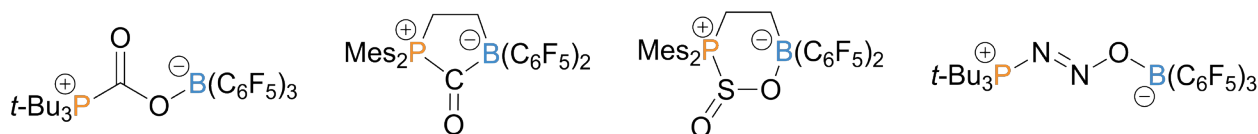
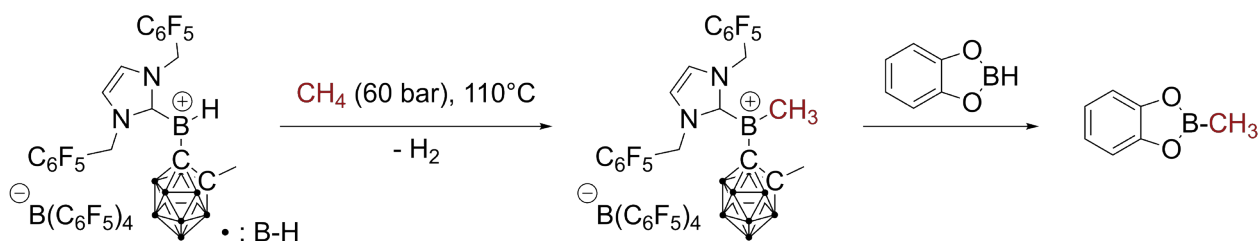


Figure 4. CO_2 , CO , SO_2 and N_2O molecules captured by FLPs.



Scheme 14. Activation and borylation of methane by a borenium complex.

under harsh conditions. A first proof of concept that CO₂ can be hydrogenated into methanol in low yield with a FLP in stoichiometric amount was described [118] by Ashley but ultimately led to the destruction of the FLP catalyst. Another stoichiometric reaction was reported by Stephan and Fontaine in 2015 [119]. More recent computational investigations hinted at the feasibility of the catalytic transformation of CO₂ into formic acid by FLPs, which is encouraging [120-122]. Eventually, Stephan's group reported the hydrogenation of CO₂ with H₂ in the presence of silyl halides, leading selectively to either disilyl acetals or methoxysilanes [123].

Another compound of great interest that cannot yet be activated by FLPs is methane (CH₄). Methane is, alongside carbon dioxide, one of the major gases responsible for global warming and its conversion into value-added products would be most profitable. Again, transition metals proved to be efficient catalysts for this challenging transformation. Periana and coworkers developed the first catalytic conversion of methane into a methanol derivative using a Pt (II) complex [124]. More recently, the groups of Sanford and Mindiola developed catalytic C-H borylations of methane using Ir, Rh and Ru complexes [125-126].

FLPs were obvious candidates for developing metal-free alternatives for the activation of methane. However, while carbon dioxide displays some reactivity with FLP systems, no reaction with methane was reported to this day. Several theoretical studies tried to address this problem by understanding the reasons behind

this difficulty: they concluded that the lack of reactivity with FLP systems is mainly due to a substantial barrier of activation, resulting from unfavorable structural reorganizations in the CH₄ moiety and the Lewis acids during the reaction, and also to weaker orbital interactions with the FLP system compared to H₂ and CO₂ [79, 127-129]. Alternatively, the group of Wang reported more recently that the activation and functionalization of methane can be achieved with a borenium cation complex, effecting its borylation (Scheme 14) and its addition on a silyl acetylene, demonstrating that reactivity with methane is possible without transition metal complexes [130].

As shown in above-detailed examples, the hydrogenation of, or the reactivity with, new and challenging substrates is strongly reliant on the development of new Lewis acids and Lewis bases, specifically designed to address limitations in the field [131-133]. In parallel, it is also crucial to understand these limitations and the parameters affecting their reactivity, for which quantum chemical calculations are necessary. Phosphines are ideal Lewis base candidates in FLP chemistry and were widely used and studied in this field [36, 134]. Their development is an important field of research, especially since they can also be applied as ligands in organometallic chemistry.

1.3. Aim of the project: merging FLP and 9-phospha-9-triptycene chemistry

An understudied and yet promising class of phosphines are 9-phospha-9-triptycene derivatives. The 9-phospha-9-triptycene (**15**, Figure 5) is a

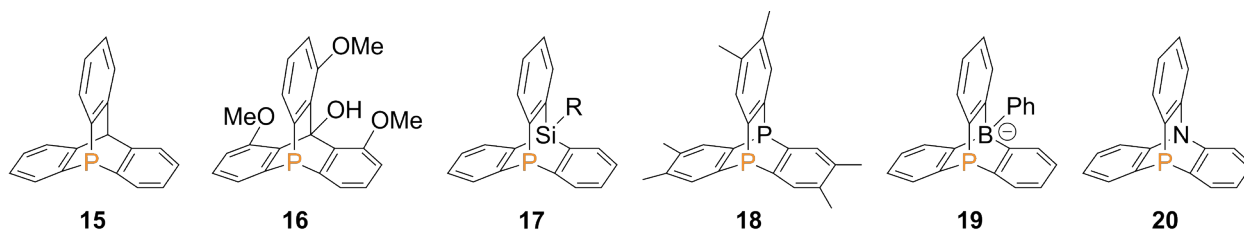


Figure 5. Phosphatriptycene **15** and reported derivatives **16-20** [142-143].

strongly pyramidalized ring-strained phosphine with its phosphorus atom in the bridgehead 9-position of the tricyclic [2.2.2]-octatriene inner motif. While heteroderivatives of the triptycene were synthesized in the decades following the parent triptycene, they found little applications until their use as ligands in the early 2000's [135-137]. Among them, the 9-phosphatriptycene was first synthesized in 1974 by Bickelhaupt in five steps with 3% overall yield [136].

In the past two decades, several new developments and syntheses were made on the phosphatriptycene and its derivatives. A new synthetic pathway was designed by the group of Kawashima in 2003 that uses phosphatriptycene oxide intermediates to access methoxy substituted phosphatriptycenes (**16**, Figure 5) [138]. Other oxide derivatives were later described by the same group [139]. Tsuji, Tamao *et al.* reported the synthesis of new 9-phospha-10-silatriptycenes **17** and derivatives as well as a study of their structure and properties [140]. In order to have a better solubility in common organic solvents, the group of Mazaki introduced methyl groups on phosphorus- and antimony-based diheteratriptycenes [141]. These methyl groups were added on the 2, 3, 6, 7, 12 and 13-positions (**18**). A significantly greater challenge, however, is to add substituents in positions 1, 8 and 14 (*i.e.* in *ortho*-position relative to the phosphorus), and no example of triptycenes with this interesting substitution pattern has been reported so far.

The parent 9-phosphatriptycene was never reportedly tested as a Lewis base in FLPs or

in any other organocatalysis. It possesses however interesting properties relevant to these applications. The scaffold is very robust and can be heated to high temperatures without degradation. Adding substituents in *ortho*-position to the phosphorus allows to tune both the electronic and steric properties of the phosphine, which is helpful in the context of FLP chemistry.

My PhD thesis aimed at developing and studying 9-phosphatriptycene derivatives and probe their application in FLP chemistry. More specifically, the goal of this investigation was to develop our fundamental understanding of structure-property relationships in cage-shaped phosphines, especially at the electronic level, while targeting applied objectives such as finding solutions to current limitations in the field of FLP catalysis.

The FLP part of the PhD project was divided into three main objectives. First, a new synthesis to access *ortho*-substituted 9-phosphatriptycene was developed, since these compounds displayed the highest potential in FLP chemistry. Next, a fundamental investigation of the steric and electronic properties was undertaken, shedding light into the parameters affecting the reactivity of these phosphines. In addition, a DFT tool to accurately predict their pK_a was developed, highlighting their weak basicity compared to regular triarylphosphines. Finally, 9-phosphatriptycenes were used for the first time as Lewis bases in FLP catalysis, taking advantage of their weak basicity to allow the hydrogenation of unactivated olefins, a challenging family of substrates.

2. Synthesis, study and application of 9-phosphatriptycenes to FLP chemistry

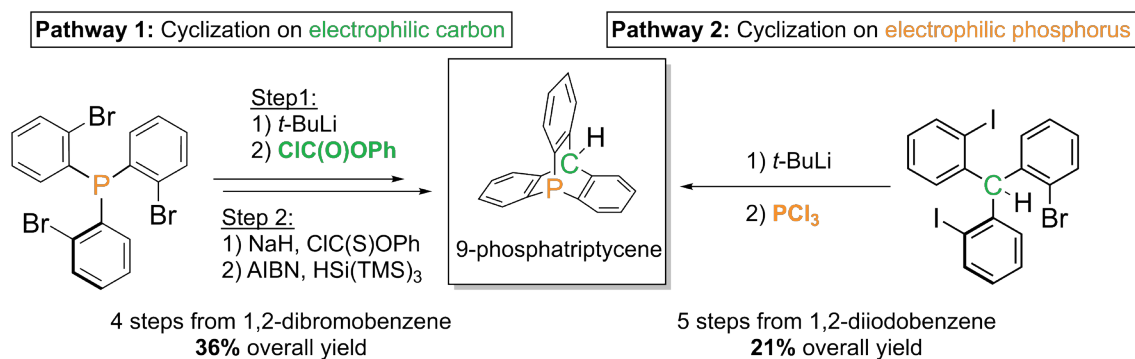
2.1. Synthesis of *ortho*-substituted 9-phosphatriptycenes

In 2018, our group published two new synthetic approaches to the parent 9-phosphatriptycene (**15**), as well as a combined experimental and theoretical investigation of its steric and electronic properties [144]. On the one hand, it can be obtained *via* an *ortho*-tribrominated phosphine precursor that undergoes a triple lithium-halogen exchange, then cyclizes on phenylchloroformate to give a 9-phospha-10-hydroxytriptycene that is further reduced into the target 9-phosphatriptycene in two steps using a Barton-McCombie deoxygenation (Scheme 15, Pathway 1). On the other hand, a trihalogenated triphenylmethane precursor [145] can be used for lithiation and cyclization on a phosphorus-based electrophile, namely PCl_3 , to obtain 9-phosphatriptycene (Scheme 15, Pathway 2).

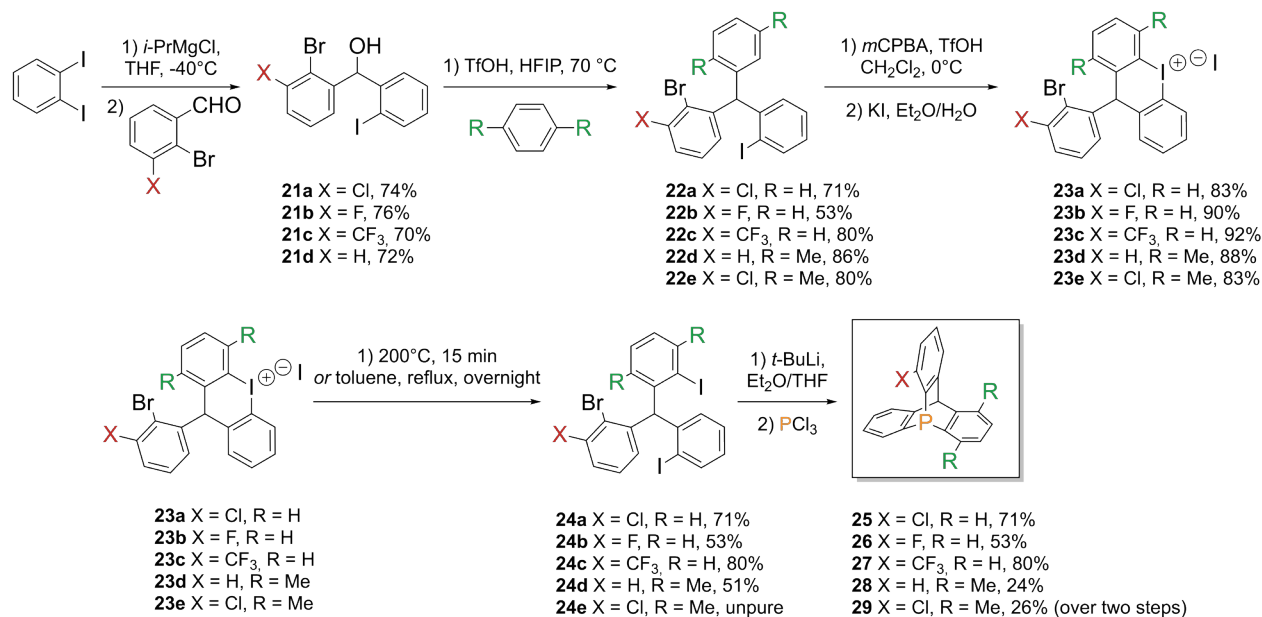
A new five-step synthesis to access *ortho*-substituted 9-phosphatriptycenes was developed during my PhD, starting from and adapting the strategy based on triphenylmethane precursors mentioned above (Scheme 16) [146]. While the synthesis based on phosphine precursors is

more efficient for the parent compound (Scheme 15), it failed at yielding *ortho*-substituted derivatives due to intermediates with excessive steric strain. The alternative strategy involving triarylmethane precursors was used instead and is detailed below.

Starting from 1,2-diiodobenzene, iodine/magnesium exchange by *i*-PrMgCl and reaction with 2-bromo-3-chlorobenzaldehyde yielded the diphenylmethanol derivative **21a**. Following a modified procedure of Moran [147], a Friedel-Crafts reaction with benzene produced **22a**. Next, iodine oxidation with *m*CPBA, intramolecular $\text{S}_{\text{E}}\text{Ar}$ and triflate/iodide anion metathesis generated the iodonium salt **23a**. Heating of the later, either neat at 200°C for 15-20 min or overnight in refluxing toluene yields trihalogenated triphenylmethane precursor **24a**. Other substituted derivatives can be obtained with the same method, either by changing the starting aldehyde (X = F, CF_3 to yield **26** and **27**) and/or using *para*-xylene instead of benzene for the Friedel-Crafts reaction (R = Me, yielding **28** and **29**). For the first time, *ortho*-substituted 9-phosphatriptycenes were synthetically accessible, which is the first step in applying their reactivity to catalysis.



Scheme 15. Formation of 9-phosphatriptycene via two synthetic pathways.



Scheme 16. Synthesis of ortho-substituted 9-phosphatriptycene derivatives. This synthesis was developed in collaboration with Dr. Lei Hu.

2.2. Reactivity study of 9-phosphatriptycenes

The choice of 9-phosphatriptycenes as Lewis base candidates in FLP catalysis is strategic not only due to their tunable steric hindrance but also due to their intrinsic reactivity. The cage-like structure of the 9-phosphatriptycene **15** and its derivatives **25-29** imposes a strong pyramidalization on the phosphorus center with respect to other triarylphosphines. This structural constraint impacts the electronic configuration of the phosphorus and induces a high *s* character of its lone pair. Interestingly, it was highlighted that this triptycene scaffold effected a weakening of the Lewis basicity of the phosphorus atom compared to the reference triphenylphosphine (PPh₃). This was evidenced experimentally by the evaluation of the Lewis Basicity (*LB*) parameter, as introduced by Mayr, with a *LB* value of 7.63 for **15** with respect to 14.27 for PPh₃, corresponding to a $\sim 10^6$ times weaker Lewis basicity towards C-centered Lewis acids [148-149].

In a recent investigation, the low basicity of 9-phosphatriptycenes was highlighted computationally by the accurate prediction of their conjugate phosphonium *pK_a* in water and acetonitrile [150]. Since Lewis bases react

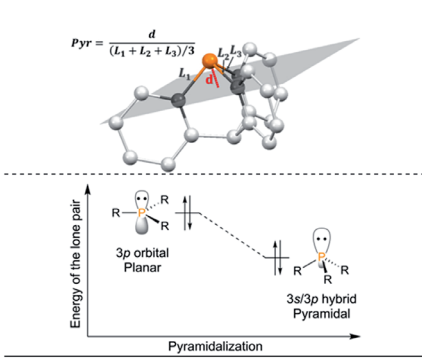
in FLP hydrogenations by the proton transfer from their conjugate acid (Scheme 6), the appropriate reactivity parameter to consider for characterization is their *pK_a*. This prediction method is based on the DFT (M06-2X/6-311G[d] with IEFPCM solvation for water or acetonitrile) determination of ΔpK_a 's improved by correlation with experimental values from the literature [151-152] (RMSD = 0.2 and 0.5 *pK_a* units in water and acetonitrile respectively). The reactivity investigation, supported by NBO calculations yielding information on the electronic state of the phosphorus atom (*e.g.* the hybridization of its orbitals), shed light into the origin of the low basicity of 9-phosphatriptycenes. As the phosphorus atom is constrained into the triptycene scaffold, its pyramidalization (pyramidalization parameter, defined below) increases relative to non-strained phosphines, resulting in an increase of the P lone pair 3*s* character (see Welsh diagram below). Since 3*s* orbitals are more stable than 3*p* orbitals, the global energy of the phosphorus lone pair is reduced and so is its reactivity, explaining the significantly lower *pK_a* predicted for these compounds. Then, changing the *ortho*-substituents allows to further fine-tune the reactivity of the phosphine. Table 1 summarizes the *pK_a* values and main NBO results highlighting this pattern.

2.3. Application to FLP catalysis

In FLP catalysis, deactivated Lewis bases find applications in the hydrogenation of weakly reactive substrates such as olefins. Since the base is weak, its conjugate acid (obtained after H₂ activation) is strong, more prone to protonate weakly reactive substrates. Still, “unactivated” olefins, such as aliphatic alkenes, are still a challenge. In a first FLP application studied in this project, 9-phosphatriptycenes were shown to be able to hydrogenate 1,1-diphenylethylene at room temperature, a reaction already reported in the literature, but serving as a proof of concept that such phosphines can serve as Lewis bases

in FLP catalysis [150]. More interestingly, 9-phosphatriptycenes derivatives allowed for the first time the hydrogenation of unactivated alkenes with an FLP catalyst: after optimization of the catalyst and the conditions, the combination of tris(pentafluorophenyl)borane (BCF) as Lewis acid and 1-chloro-9-phosphatriptycene as Lewis base reduced cyclohexene to cyclohexane at 150°C overnight under high dihydrogen pressure (40 bar) with up to 88% yield (Scheme 17) [153].

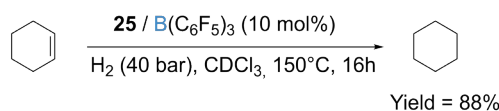
Comparison with other deactivated Lewis bases highlighted the effect of the triptycene scaffold on the phosphorus reactivity since no other phosphine was able to catalyze this reaction as



Phosphines	Est. p <i>K</i> _a (MeCN)	Est. p <i>K</i> _a (H ₂ O)	ε _{LP} (eV)	<i>Pyr</i>	3 <i>s</i> _{LP} (%)	3 <i>p</i> _{LP} (%)
PPh₃	7.62 ^[a]	3.28 ^[a]	-11.66	0.452	45.4	54.6
15 (-H)	-0.7	-2.9	-12.78	0.536	49.9	50.1
25 (-Cl)	-2.6	-4.2	-12.95	0.538	50.8	49.2
26 (-F)	-2.5	-4.1	-12.93	0.540	50.7	49.3
27 (-CF ₃)	-2.9	-4.5	-12.99	0.538	50.9	49.1
28 (-Xyl)	0.2	-2.2	-12.71	0.534	49.9	50.1
29 (Cl, Xyl)	-1.5	-3.5	-12.88	0.536	50.8	49.2

[a] Experimental values.

Table 1. Estimated (Est.) p*K*_a's in acetonitrile (MeCN) and water (H₂O) of the conjugate phosphonium of selected phosphines, pyramidalization parameter (*Pyr*), energy of the phosphorus lone pair (ε_{LP}), its 3*s* and 3*p* characters.



Scheme 17. Optimized conditions for the hydrogenation of cyclohexene with 1-chloro-9-phosphatriptycene **25** and BCF. NMR yield indicated.

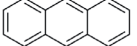
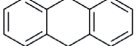
Entry	Substrate	Product	Conversion (%) ^[a]	¹ H NMR yield (%) ^[a]
1			100	72
2			100	60
3			100	70
4			84	76
5			61 ^[b]	57 ^[b]
6			0	0
7			33	20
8			26	3

Table 2. Substrate scope of hydrogenation with 1-chloro-9-phosphatriptycene **25** and BCF as catalyst.

Conditions: 10 mol% catalyst, Solvent= CDCl₃, 150°C, 16h, 40 bar H₂. [a] Triphenylmethane or 1,3,5-trimethoxybenzene used as ¹H NMR internal standard for yield determination. [b] Reaction time increased to 72h.

effectively, even the ones bearing deactivating groups, such as P(2-Br-C₆H₄)₃, P(4-Cl-C₆H₄)₃ or P(C₆F₅)Ph₂. Eventually, a scope of substrates was undertaken, showing that these conditions tolerate cyclic and acyclic olefins, even the ones bearing deactivating groups, but steric hindrance in the substrate hampers the reaction (Table 2). So far thus, substrates are limited to mono- and di-substituted olefins, or trisubstituted ones with limited steric hindrance.

Inserting phosphorus into the triptycene scaffold and using 9-phosphatriptycene as organocatalysts thus solved a lasting issue in FLP catalysis, namely the hydrogenation of unactivated alkenes. In addition to this applied outcome, it is also a fundamental proof of concept that targeting the structure of main group elements such a phosphorus is an effective but underdeveloped tool that can be used in combination with the usual strategy consisting in changing the nature and number of substituents (*i.e.* electron-withdrawing or -donating groups).

3. Conclusions

Frustrated Lewis pair chemistry opened a new door in acid-base reactivity and catalysis. Over

the years, from the definition of early concepts to deeper mechanistic and scope investigations, this new field of organocatalysis has developed very quickly. Currently, the synthesis of new Lewis acids and bases is inherent to solving limitations in metal-free catalysis, such as the hydrogenation of unactivated alkenes. In this context, 9-phosphatriptycenes are appealing solutions since they display both the steric hindrance necessary for FLP reactivity and the weak basicity necessary for the hydrogenation of less reactive substrates. My PhD project allowed to expand the reactivity of FLP catalyst with the use of 9-phosphatriptycenes. A new synthesis giving access to a series of *ortho*-substituted derivatives was developed. Then a reactivity investigation to understand the origin of their weak basicity was undertaken, showing that the increased pyramidalization of the phosphine due to the triptycene scaffold stabilizes the phosphorus lone pair, resulting in a weaker reactivity. Finally, the high acidity of the conjugate phosphonium of 9-phosphatriptycenes was taken advantage of to allow for the first time the hydrogenation of unactivated alkenes by FLP catalysis.

References

- [1] G. N. Lewis, *Valence and the structure of atoms and molecules*, American Chemical Society, **1923**.
- [2] H. C. Brown, H. I. Schlesinger, S. Z. Cardon, "Studies in stereochemistry. I. Steric strains as a factor in the relative stability of some coordination compounds of boron", *J. Am. Chem. Soc.* **1942**, *64*, 325-329.
- [3] G. C. Welch, R. R. San Juan, J. D. Masuda, D. W. Stephan, "Reversible, metal-free hydrogen activation", *Science* **2006**, *314*, 1124-1126.
- [4] G. C. Welch, D. W. Stephan, "Facile heterolytic cleavage of dihydrogen by phosphines and boranes", *J. Am. Chem. Soc.* **2007**, *129*, 1880-1881.
- [5] D. W. Stephan, "'frustrated Lewis pairs': A concept for new reactivity and catalysis", *Org. Biomol. Chem.* **2008**, *6*, 1535-1539.
- [6] J. S. McCahill, G. C. Welch, D. W. Stephan, "Reactivity of 'frustrated Lewis pairs': three-component reactions of phosphines, a borane, and olefins", *Angew. Chem. Int. Ed.* **2007**, *46*, 4968-4971.
- [7] P. A. Chase, G. C. Welch, T. Jurca, D. W. Stephan, "Metal-free catalytic hydrogenation", *Angew. Chem. Int. Ed.* **2007**, *46*, 8050-8053.
- [8] D. W. Stephan, "'Frustrated Lewis pair' hydrogenations", *Org. Biomol. Chem.* **2012**, *10*, 5740-5746.
- [9] C. H. Bartholomew, R. J. Farrauto, *Fundamentals of industrial catalytic processes*, 2nd ed., John Wiley & sons, Inc., Hoboken (NJ), USA, **2006**.
- [10] H.-U. Blaser, C. Malan, B. Pugin, F. Spindler, H. Steiner, M. Studer, "Selective hydrogenation for fine chemicals: recent trends and new developments", *Adv. Synth. Catal.* **2003**, *345*, 103-151.
- [11] P. Sabatier, "How I have been led to the direct hydrogenation method by metallic catalysts", *Ind. Eng. Chem.* **1926**, *18*, 1005-1008.
- [12] J. G. de Vries, C. J. Elsevier (Ed.), *The handbook of homogeneous hydrogenation*, Wiley-VCH, Weinheim, **2006**.
- [13] R. H. Crabtree (Ed.), *The organometallic chemistry of the transition metals*, 6th ed., John Wiley & Sons, Inc., Hoboken, **2014**.
- [14] R. Morris Bullock (Ed.), *Catalysis without precious metals*, Wiley-VCH, Weinheim, Germany, **2010**.
- [15] B. K. Sovacool, S. H. Ali, M. Bazilian, B. Radley, B. Nemery, J. Okatz, D. Mulvaney, "Sustainable minerals and metals for a low-carbon future", *Science* **2020**, *367*, 30-33.
- [16] E. Lebre, M. Stringer, K. Svobodova, J. R. Owen, D. Kemp, C. Cote, A. Arratia-Solar, R. K. Valenta, "The social and environmental complexities of extracting energy transition metals", *Nature Communications* **2020**, *11*, 4823.
- [17] K. S. Egorova, V. P. Ananikov, "Toxicity of metal compounds: knowledge and myths", *Organometallics* **2017**, *36*, 4071-4090.
- [18] W. Cheves, L. Bollyky, "Homogeneous hydrogenation in the absence of transition-metal catalysts", *J. Am. Chem. Soc.* **1964**, *86*, 3750-3752.
- [19] A. Berkessel, T. J. Schubert, T. N. Muller, "Hydrogenation without a transition-metal catalyst: on the mechanism of the base-catalyzed hydrogenation of ketones", *J. Am. Chem. Soc.* **2002**, *124*, 8693-8698.
- [20] P. I. Dalko, L. Moisan, "In the golden age of organocatalysis", *Angew. Chem. Int. Ed.* **2004**, *43*, 5138-5175.
- [21] J. W. Yang, M. T. Hechavarria Fonseca, B. List, "A metal-free transfer hydrogenation: organocatalytic conjugate reduction of alpha,beta-unsaturated aldehydes", *Angew. Chem. Int. Ed.* **2004**, *43*, 6660-6662.
- [22] H. Adolfsson, "Organocatalytic hydride transfers: a new concept in asymmetric hydrogenations", *Angew. Chem. Int. Ed.* **2005**, *44*, 3340-3342.
- [23] M. Rueping, A. P. Antonchick, T. Theissmann, "A highly enantioselective Brønsted acid catalyzed cascade reaction: organocatalytic transfer hydrogenation of quinolines and their application in the synthesis of alkaloids", *Angew. Chem. Int. Ed.* **2006**, *45*, 3683-3686.
- [24] J. B. Tuttle, S. G. Ouellet, D. W. MacMillan, "Organocatalytic transfer hydrogenation of cyclic enones", *J. Am. Chem. Soc.* **2006**, *128*, 12662-12663.
- [25] C. Zheng, S. L. You, "Transfer hydrogenation with Hantzsch esters and related organic hydride donors", *Chem. Soc. Rev.* **2012**, *41*, 2498-2518.
- [26] J. Paradies, "Frustrated Lewis pair catalyzed hydrogenations", *Synlett* **2013**, *24*, 777-780.
- [27] J. Lam, K. M. Szkop, E. Mosaferi, D. W. Stephan, "FLP catalysis: main group hydrogenations of organic unsaturated substrates", *Chem. Soc. Rev.* **2019**, *48*, 3592-3612.
- [28] J. Paradies, Z. P. Tavandashti, R. Zhou, "Frustrated Lewis Pair Catalyzed Reactions", *SynOpen* **2023**, *07*, 46-57.
- [29] P. A. Chase, T. Jurca, D. W. Stephan, "Lewis acid-catalyzed hydrogenation: B(C₆F₅)₃-mediated reduction of imines and nitriles with H₂", *Chem. Commun.* **2008**, 1701-1703.
- [30] D. Chen, J. Klankermayer, "Metal-free catalytic hydrogenation of imines with tris(perfluorophenyl) borane", *Chem. Commun.* **2008**, 2130-2131.
- [31] P. Spies, S. Schwendemann, S. Lange, G. Kehr, R. Frohlich, G. Erker, "Metal-free catalytic hydrogenation of enamines, imines, and conjugated phosphinoalkenylboranes", *Angew. Chem. Int. Ed.* **2008**, *47*, 7543-7546.
- [32] G. Erös, K. Nagy, H. Mehdi, I. Pápai, P. Nagy, P. Király, G. Tárkányi, T. Soős, "Catalytic hydrogenation with frustrated Lewis pairs: Selectivity achieved by size-exclusion design of Lewis acids", *Chem. Eur. J.* **2012**, *18*, 574-585.
- [33] V. Sumerin, F. Schulz, M. Atsumi, C. Wang, M. Nieger, M. Leskela, T. Repo, P. Pykko, B. Rieger, "Molecular tweezers for hydrogen: synthesis, characterization, and reactivity", *J. Am. Chem. Soc.* **2008**, *130*, 14117-14119.
- [34] S. Tussing, L. Greb, S. Tamke, B. Schirmer, C. Muhle-Goll, B. Luy, J. Paradies, "Autoinduced catalysis and inverse equilibrium isotope effect in the frustrated Lewis pair catalyzed hydrogenation of imines", *Chem. Eur. J.* **2015**, *21*, 8056-8059.
- [35] D. J. Scott, M. J. Fuchter, A. E. Ashley, "Metal-free hydrogenation catalyzed by an air-stable borane: use of solvent as a frustrated Lewis base", *Angew. Chem. Int. Ed.* **2014**, *53*, 10218-10222.
- [36] L. Greb, P. Oña-Burgos, B. Schirmer, S. Grimme, D. W. Stephan, J. Paradies, "Metal-free catalytic olefin hydrogenation: Low-temperature H₂ activation by frustrated Lewis pairs", *Angew. Chem. Int. Ed.* **2012**, *51*, 10164-10168.

- [37] L. J. Hounjet, C. Bannwarth, C. N. Garon, C. B. Caputo, S. Grimme, D. W. Stephan, "Combinations of ethers and $B(C_6F_5)_3$ function as hydrogenation catalysts", *Angew. Chem. Int. Ed.* **2013**, *52*, 7492-7495.
- [38] S. J. Geier, P. A. Chase, D. W. Stephan, "Metal-free reductions of N-heterocycles via Lewis acid catalyzed hydrogenation", *Chem. Commun.* **2010**, *46*, 4884-4886.
- [39] Y. Segawa, D. W. Stephan, "Metal-free hydrogenation catalysis of polycyclic aromatic hydrocarbons", *Chem. Commun.* **2012**, *48*, 11963-11965.
- [40] T. Mahdi, Z. M. Heiden, S. Grimme, D. W. Stephan, "Metal-free aromatic hydrogenation: Aniline to cyclohexyl-amine derivatives", *J. Am. Chem. Soc.* **2012**, *134*, 4088-4091.
- [41] G. Li, Y. Liu, H. Du, " $B(C_6F_5)_3$ -catalyzed metal-free hydrogenation of naphthylamines", *Org. Biomol. Chem.* **2015**, *13*, 2875-2878.
- [42] B. Ines, D. Palomas, S. Holle, S. Steinberg, J. A. Nicasio, M. Alcarazo, "Metal-free hydrogenation of electron-poor allenes and alkenes", *Angew. Chem. Int. Ed.* **2012**, *51*, 12367-12369.
- [43] J. A. Nicasio, S. Steinberg, B. Ines, M. Alcarazo, "Tuning the Lewis acidity of boranes in frustrated Lewis pair chemistry: implications for the hydrogenation of electron-poor alkenes", *Chem. Eur. J.* **2013**, *19*, 11016-11020.
- [44] L. Greb, C. G. Daniliuc, K. Bergander, J. Paradies, "Functional-group tolerance in frustrated Lewis pairs: hydrogenation of nitroolefins and acrylates", *Angew. Chem. Int. Ed.* **2013**, *52*, 5876-5879.
- [45] Y. Wang, W. Chen, Z. Lu, Z. H. Li, H. Wang, "Metal-free $HB(C_6F_5)_2$ -catalyzed hydrogenation of unfunctionalized olefins and mechanism study of borane-mediated σ -bond metathesis", *Angew. Chem. Int. Ed.* **2013**, *52*, 7496-7499.
- [46] F. L. Ramp, E. J. DeWitt, L. E. Trapasso, "Homogeneous hydrogenation catalyzed by boranes", *J. Am. Chem. Soc.* **1961**, *83*, 4672.
- [47] F. L. Ramp, E. J. DeWitt, L. E. Trapasso, "Homogeneous hydrogenation catalyzed by boranes", *J. Org. Chem.* **1962**, *27*, 4368-4372.
- [48] D. J. Parks, W. E. Piers, G. P. A. Yap, "Synthesis, properties, and hydroboration activity of the highly electrophilic borane bis(pentafluorophenyl)borane, $HB(C_6F_5)_2$ ", *Organometallics* **1998**, *17*, 5492-5503.
- [49] B. H. Xu, G. Kehr, R. Frohlich, B. Wibbeling, B. Schirmer, S. Grimme, G. Erker, "Reaction of frustrated Lewis pairs with conjugated ynones-selective hydrogenation of the carbon-carbon triple bond", *Angew. Chem. Int. Ed.* **2011**, *50*, 7183-7186.
- [50] K. Chernichenko, A. Madarasz, I. Papp, M. Nieger, M. Leskela, T. Repo, "A frustrated-Lewis-pair approach to catalytic reduction of alkynes to *cis*-alkenes", *Nat. Chem.* **2013**, *5*, 718-723.
- [51] Y. Liu, L. Hu, H. Chen, H. Du, "An alkene-promoted borane-catalyzed highly stereoselective hydrogenation of alkynes to give *Z*- and *E*-alkenes", *Chem. Eur. J.* **2015**, *21*, 3495-3501.
- [52] J. Nyhlen, T. Privalov, "On the possibility of catalytic reduction of carbonyl moieties with tris(pentafluorophenyl)borane and H_2 : a computational study", *Dalton Trans.* **2009**, 5780-5786.
- [53] M. Lindqvist, N. Sarnela, V. Sumerin, K. Chernichenko, M. Leskela, T. Repo, "Heterolytic dihydrogen activation by $B(C_6F_5)_3$ and carbonyl compounds", *Dalton Trans.* **2012**, *41*, 4310-4312.
- [54] L. E. Longobardi, C. Tang, D. W. Stephan, "Stoichiometric reductions of alkyl-substituted ketones and aldehydes to borinic esters", *Dalton Trans.* **2014**, *43*, 15723-15726.
- [55] D. J. Scott, M. J. Fuchter, A. E. Ashley, "Non-metal catalyzed hydrogenation of carbonyl compounds", *J. Am. Chem. Soc.* **2014**, *136*, 15813-15816.
- [56] T. Mahdi, D. W. Stephan, "Enabling catalytic ketone hydrogenation by frustrated Lewis pairs", *J. Am. Chem. Soc.* **2014**, *136*, 15809-15812.
- [57] G. Erős, H. Mehdi, I. Pápai, T. A. Rokob, P. Király, G. Tárkányi, T. Soós, "Expanding the scope of metal-free catalytic hydrogenation through frustrated Lewis pair design", *Angew. Chem. Int. Ed.* **2010**, *122*, 6709-6713.
- [58] É. Dorkó, M. Szabó, B. Kótai, I. Pápai, A. Domján, T. Soós, "Expanding the boundaries of water-tolerant frustrated Lewis pair hydrogenation: Enhanced back strain in the Lewis acid enables the reductive amination of carbonyls", *Angew. Chem. Int. Ed.* **2017**, *56*, 9512-9516.
- [59] Á. Gyömöre, M. Bakos, T. Földes, I. Pápai, A. Domján, T. Soós, "Moisture-tolerant frustrated Lewis pair catalyst for hydrogenation of aldehydes and ketones", *ACS Catal.* **2015**, *5*, 5366-5372.
- [60] A. M. Smith, R. Whyman, "Review of methods for the catalytic hydrogenation of carboxamides", *Chem. Rev.* **2014**, *114*, 5477-5510.
- [61] N. A. Sitte, M. Bursch, S. Grimme, J. Paradies, "Frustrated Lewis pair catalyzed hydrogenation of amides: halides as active Lewis base in the metal-free hydrogen activation", *J. Am. Chem. Soc.* **2019**, *141*, 159-162.
- [62] H. Zhu, Z. W. Qu, S. Grimme, "Borane-catalyzed hydrogenation of tertiary amides activated by oxalyl chloride: DFT mechanistic insights", *Eur. J. Org. Chem.* **2019**, *2019*, 4609-4612.
- [63] L. Koring, N. A. Sitte, M. Bursch, S. Grimme, J. H. H. Paradies, "Hydrogenation of secondary amides using phosphane oxide and frustrated Lewis pair catalysis", *Chem. Eur. J.* **2021**.
- [64] J. S. Sapsford, D. Csókás, R. C. Turnell-Ritson, L. A. Parkin, A. D. Crawford, I. Pápai, A. E. Ashley, "Transition metal-free direct hydrogenation of esters via a frustrated Lewis pair", *ACS Catal.* **2021**, 9143-9150.
- [65] D. Chen, Y. Wang, J. Klankermayer, "Enantioselective hydrogenation with chiral frustrated Lewis pairs", *Angew. Chem. Int. Ed.* **2010**, *49*, 9475-9478.
- [66] G. Ghattas, D. Chen, F. Pan, J. Klankermayer, "Asymmetric hydrogenation of imines with a recyclable chiral frustrated Lewis pair catalyst", *Dalton Trans.* **2012**, *41*, 9026-9028.
- [67] X. Wang, G. Kehr, C. G. Daniliuc, G. Erker, "Internal adduct formation of active intramolecular C_4 -bridged frustrated phosphane/borane Lewis pairs", *J. Am. Chem. Soc.* **2014**, *136*, 3293-3303.
- [68] K. Y. Ye, X. Wang, C. G. Daniliuc, G. Kehr, G. Erker, "A ferrocene-based phosphane/borane frustrated Lewis pair for asymmetric imine reduction", *Eur. J. Inorg. Chem.* **2016**, *2017*, 368-371.
- [69] V. Sumerin, K. Chernichenko, M. Nieger, M. Leskela, B. Rieger, T. Repo, "Highly active metal-free catalysts for hydrogenation of unsaturated nitrogen-containing compounds", *Adv. Synth. Catal.* **2011**, *353*, 2093-2110.

- [70] Y. Liu, H. Du, "Chiral dienes as "ligands" for borane-catalyzed metal-free asymmetric hydrogenation of imines", *J. Am. Chem. Soc.* **2013**, *135*, 6810-6813.
- [71] M. Lindqvist, K. Borre, K. Axenov, B. Kotai, M. Nieger, M. Leskela, I. Papai, T. Repo, "Chiral molecular tweezers: synthesis and reactivity in asymmetric hydrogenation", *J. Am. Chem. Soc.* **2015**, *137*, 4038-4041.
- [72] S. Wei, H. Du, "A highly enantioselective hydrogenation of silyl enol ethers catalyzed by chiral frustrated Lewis pairs", *J. Am. Chem. Soc.* **2014**, *136*, 12261-12264.
- [73] X. Ren, G. Li, S. Wei, H. Du, "Facile development of chiral alkenylboranes from chiral diynes for asymmetric hydrogenation of silyl enol ethers", *Org. Lett.* **2015**, *17*, 990-993.
- [74] Z. Zhang, H. Du, "Enantioselective metal-free hydrogenations of disubstituted quinolines", *Org. Lett.* **2015**, *17*, 6266-6269.
- [75] Z. Zhang, H. Du, "Cis-selective and highly enantioselective hydrogenation of 2,3,4-trisubstituted quinolines", *Org. Lett.* **2015**, *17*, 2816-2819.
- [76] Z. Zhang, H. Du, "A highly cis-selective and enantioselective metal-free hydrogenation of 2,3-disubstituted quinoxalines", *Angew. Chem. Int. Ed.* **2015**, *54*, 623-626.
- [77] T. A. Rokob, A. Hamza, A. Stirling, T. Soós, I. Pápai, "Turning frustration into bond activation: A theoretical mechanistic study on heterolytic hydrogen splitting by frustrated Lewis pairs", *Angew. Chem. Int. Ed.* **2008**, *47*, 2435-2438.
- [78] T. A. Rokob, A. Hamza, I. Pápai, "Rationalizing the reactivity of frustrated Lewis pairs: Thermodynamics of H₂ activation and the role of acid-base properties", *J. Am. Chem. Soc.* **2009**, *131*, 10701-10710.
- [79] H. Li, L. Zhao, G. Lu, Y. Mo, Z. X. Wang, "Insight into the relative reactivity of "frustrated Lewis pairs" and stable carbenes in activating H₂ and CH₄: a comparative computational study", *Phys. Chem. Chem. Phys.* **2010**, *12*, 5268-5275.
- [80] S. Gao, W. Wu, Y. Mo, "Steric and electronic effects on the heterolytic H₂-splitting by phosphine-boranes R₃B/PR'₃ (R = C₆F₅, Ph; R' = C₆H₂Me₃, tBu, Ph, C₆F₅, Me, H): a computational study", *Int. J. Quantum Chem.* **2011**, *111*, 3761-3775.
- [81] T. A. Rokob, I. Papai, "Hydrogen activation by frustrated Lewis pairs: insights from computational studies", *Top. Curr. Chem.* **2013**, *332*, 157-212.
- [82] L. L. Zeonjuk, N. Vankova, A. Mavrandonakis, T. Heine, G.-V. Rösenthaller, J. Eicher, "On the mechanism of hydrogen activation by frustrated Lewis pairs", *Chem. Eur. J.* **2013**, *19*, 17413-17424.
- [83] J. Paradies, "Mechanisms in frustrated Lewis pair-catalyzed reactions", *Eur. J. Org. Chem.* **2019**, *2019*, 283-294.
- [84] G. Sharma, P. D. Newman, J. A. Platts, "A review of quantum chemical studies of frustrated Lewis pairs", *J. Mol. Graphics Modell.* **2021**, *105*, 107846.
- [85] T. J. Tague, L. Andrews, "Reactions of pulsed-laser evaporated boron atoms with hydrogen. Infrared spectra of boron hydride intermediate species in solid argon", *J. Am. Chem. Soc.* **1994**, *116*, 4970-4976.
- [86] J. D. Watts, R. J. Bartlett, "On the existence of BH₅", *J. Am. Chem. Soc.* **1995**, *117*, 825-826.
- [87] A. Hamza, A. Stirling, T. András Rokob, I. Pápai, "Mechanism of hydrogen activation by frustrated Lewis pairs: A molecular orbital approach", *Int. J. Quantum Chem.* **2009**, *109*, 2416-2425.
- [88] Y. Guo, S. Li, "Unusual concerted Lewis acid-Lewis base mechanism for hydrogen activation by a phosphine-borane compound", *Inorg. Chem.* **2008**, *47*, 6212-6219.
- [89] S. Grimme, H. Kruse, L. Goerigk, G. Erker, "The mechanism of dihydrogen activation by frustrated Lewis pairs revisited", *Angew. Chem. Int. Ed.* **2010**, *49*, 1402-1405.
- [90] S. Grimme, "Semi-empirical GGA-type density functional constructed with a long-range dispersion correction", *J. Comput. Chem.* **2006**, *27*, 1787-1799.
- [91] A. Schäfer, C. Huber, R. Ahlrichs, "Fully optimized contracted Gaussian basis sets of triple zeta valence quality for atoms Li to Kr", *J. Chem. Phys.* **1994**, *100*, 5829-5835.
- [92] S. Grimme, "Improved second-order Møller-Plesset perturbation theory by separate scaling of parallel- and antiparallel-spin pair correlation energies", *J. Chem. Phys.* **2003**, *118*, 9095-9102.
- [93] G. A. Petersson, M. Braunstein, "Complete basis set correlation energies. IV. The total correlation energy of the water molecule", *J. Chem. Phys.* **1985**, *83*, 5129-5134.
- [94] J. W. Ochterski, G. A. Petersson, K. B. Wiberg, "A comparison of model chemistries", *J. Am. Chem. Soc.* **2002**, *117*, 11299-11308.
- [95] D. M. Camaioni, B. Ginovska-Pangovska, G. K. Schenter, S. M. Kathmann, T. Autrey, "Analysis of the activation and heterolytic dissociation of H₂ by frustrated Lewis pairs: NH₃/BX₃ (X = H, F, and Cl)", *J. Phys. Chem. A* **2012**, *116*, 7228-7237.
- [96] A. G. Baboul, L. A. Curtiss, P. C. Redfern, K. Raghavachari, "Gaussian-3 theory using density functional geometries and zero-point energies", *J. Chem. Phys.* **1999**, *110*, 7650-7657.
- [97] T. A. Rokob, I. Bako, A. Stirling, A. Hamza, I. Papai, "Reactivity models of hydrogen activation by frustrated Lewis pairs: synergistic electron transfers or polarization by electric field?", *J. Am. Chem. Soc.* **2013**, *135*, 4425-4437.
- [98] M. Pu, T. Privalov, "Ab initio dynamics trajectory study of the heterolytic cleavage of H₂ by a Lewis acid [B(C₆F₅)₃] and a Lewis base [P(tBu)₃]", *J. Chem. Phys.* **2013**, *138*, 154305.
- [99] L. Liu, B. Lukose, B. Ensing, "Hydrogen activation by frustrated Lewis pairs revisited by metadynamics simulations", *The Journal of Physical Chemistry C* **2017**, *121*, 2046-2051.
- [100] J. Daru, I. Bakó, A. Stirling, I. Pápai, "Mechanism of heterolytic hydrogen splitting by frustrated Lewis pairs: comparison of static and dynamic models", *ACS Catal.* **2019**, *9*, 6049-6057.
- [101] M. Heshmat, T. Privalov, "H₂ cleavage by frustrated Lewis pairs characterized by the energy decomposition analysis of transition states: An alternative to the electron transfer and electric field models", *J. Phys. Chem. A* **2018**, *122*, 7202-7211.
- [102] D. W. Stephan, G. Erker, "Frustrated Lewis pairs: metal-free hydrogen activation and more", *Angew. Chem. Int. Ed.* **2010**, *49*, 46-76.

- [103] D. W. Stephan, "The broadening reach of frustrated Lewis pair chemistry", *Science* **2016**, *354*, 1248-1256.
- [104] D. W. Stephan, G. Erker, "Frustrated Lewis pair chemistry of carbon, nitrogen and sulfur oxides", *Chem. Sci.* **2014**, *5*, 2625-2641.
- [105] C. M. Mömring, E. Otten, G. Kehr, R. Fröhlich, S. Grimme, D. W. Stephan, G. Erker, "Reversible metal-free carbon dioxide binding by frustrated Lewis pairs", *Angew. Chem. Int. Ed.* **2009**, *48*, 6643-6646.
- [106] M. Sajid, A. Klose, B. Birkmann, L. Liang, B. Schirmer, T. Wiegand, H. Eckert, A. J. Lough, R. Fröhlich, C. G. Daniliuc, S. Grimme, D. W. Stephan, G. Kehr, G. Erker, "Reactions of phosphorus/boron frustrated Lewis pairs with SO₂", *Chem. Sci.* **2013**, *4*, 213-219.
- [107] E. Otten, R. C. Neu, D. W. Stephan, "Complexation of nitrous oxide by frustrated Lewis pairs", *J. Am. Chem. Soc.* **2009**, *131*, 9918-9919.
- [108] A. J. P. Cardenas, B. J. Culotta, T. H. Warren, S. Grimme, A. Stute, R. Fröhlich, G. Kehr, G. Erker, "Capture of NO by a frustrated Lewis pair: a new type of persistent N-oxyl radical", *Angew. Chem. Int. Ed.* **2011**, *50*, 7567-7571.
- [109] T. R. Karl, K. E. Trenberth, "Modern global climate change", *Science* **2003**, *302*, 1719-1723.
- [110] G. A. Olah, A. Goepfert, G. K. Prakash, "Chemical recycling of carbon dioxide to methanol and dimethyl ether: from greenhouse gas to renewable, environmentally carbon neutral fuels and synthetic hydrocarbons", *J. Org. Chem.* **2009**, *74*, 487-498.
- [111] D. Mellmann, P. Sponholz, H. Junge, M. Beller, "Formic acid as a hydrogen storage material - development of homogeneous catalysts for selective hydrogen release", *Chem. Soc. Rev.* **2016**, *45*, 3954-3988.
- [112] B. Grignard, S. Gennen, C. Jérôme, A. W. Kleij, C. Detrembleur, "Advances in the use of CO₂ as a renewable feedstock for the synthesis of polymers", *Chem. Soc. Rev.* **2019**, *48*, 4466-4514.
- [113] X. Jiang, X. Nie, X. Guo, C. Song, J. G. Chen, "Recent Advances in Carbon Dioxide Hydrogenation to Methanol via Heterogeneous Catalysis", *Chem. Rev.* **2020**, *120*, 7984-8034.
- [114] W. Taifan, J. F. Boily, J. Baltrusaitis, "Surface chemistry of carbon dioxide revisited", *Surf. Sci. Rep.* **2016**, *71*, 595-671.
- [115] C. Costentin, M. Robert, J. M. Savéant, "Catalysis of the electrochemical reduction of carbon dioxide", *Chem. Soc. Rev.* **2013**, *42*, 2423-2436.
- [116] R. Tanaka, M. Yamashita, K. Nozaki, "Catalytic hydrogenation of carbon dioxide using Ir(III)-pincer complexes", *J. Am. Chem. Soc.* **2009**, *131*, 14168-14169.
- [117] T. Zhao, X. Hu, Y. Wu, Z. Zhang, "Hydrogenation of CO₂ to formate with H₂: Transition metal free catalyst based on a Lewis pair", *Angew. Chem. Int. Ed.* **2019**, *58*, 722-726.
- [118] A. E. Ashley, A. L. Thompson, D. O'Hare, "Non-metal-mediated homogeneous hydrogenation of CO₂ to CH₃OH", *Angew. Chem. Int. Ed.* **2009**, *48*, 9839-9843.
- [119] M.-A. Courtemanche, A. P. Pulis, É. Rochette, M.-A. Légaré, D. W. Stephan, F.-G. Fontaine, "Intramolecular B/N frustrated Lewis pairs and the hydrogenation of carbon dioxide", *Chem. Commun.* **2015**, *51*, 9797-9800.
- [120] L. Liu, N. Vankova, T. Heine, "A kinetic study on the reduction of CO₂ by frustrated Lewis pairs: from understanding to rational design", *Phys. Chem. Chem. Phys.* **2016**, *18*, 3567-3574.
- [121] B. Jiang, Q. Zhang, L. Dang, "Theoretical studies on bridged frustrated Lewis pair (FLP) mediated H₂ activation and CO₂ hydrogenation", *Organic Chemistry Frontiers* **2018**, *5*, 1905-1915.
- [122] M. Ghara, P. K. Chattaraj, "A computational study on hydrogenation of CO₂, catalyzed by a bridged B/N frustrated Lewis pair", *Struct. Chem.* **2019**, *30*, 1067-1077.
- [123] T. Wang, M. Xu, A. R. Jupp, Z. W. Qu, S. Grimme, D. W. Stephan, "Selective catalytic frustrated Lewis pair hydrogenation of CO₂ in the presence of silylhalides", *Angew. Chem. Int. Ed.* **2021**, *60*, 25771-25775.
- [124] R. A. Periana, D. J. Taube, S. Gamble, H. Taube, T. Satoh, H. Fujii, "Platinum catalysts for the high-yield oxidation of methane to a methanol derivative", *Science* **1998**, *280*, 560-564.
- [125] A. K. Cook, S. D. Schimler, A. J. Matzger, M. S. Sanford, "Catalyst-controlled selectivity in the C-H borylation of methane and ethane", *Science* **2016**, *351*, 1421-1424.
- [126] K. T. Smith, S. Berritt, M. González-Moreiras, S. Ahn, M. R. Smith, M. H. Baik, D. J. Mindiola, "Catalytic borylation of methane", *Science* **2016**, *351*, 1424-1427.
- [127] S. Frömel, C. G. Daniliuc, C. Bannwarth, S. Grimme, K. Bussmann, G. Kehr, G. Erker, "Indirect synthesis of a pair of formal methane activation products at a phosphane/borane frustrated Lewis pair", *Dalton Trans.* **2016**, *45*, 19230-19233.
- [128] N. Villegas-Escobar, A. Toro-Labbé, M. Becerra, M. Real-Enriquez, J. R. Mora, L. Rincon, "A DFT study of hydrogen and methane activation by B(C₆F₅)₃/P(t-Bu)₃ and Al(C₆F₅)₃/P(t-Bu)₃ frustrated Lewis pairs", *J. Mol. Model.* **2017**, *23*.
- [129] D. Mahaut, A. Chardon, L. Mineur, G. Berionni, B. Champagne, "Rational development of a metal-free bifunctional system for the C-H activation of methane: a density functional theory investigation", *ChemPhysChem* **2021**, *22*, 1958-1966.
- [130] Y. Liu, W. Dong, Z. H. Li, H. Wang, "Methane activation by a borenium complex", *Chem* **2021**, *7*, 1843-1851.
- [131] S. Mukherjee, P. Thilagar, "Frustrated Lewis pairs: Design and reactivity", *Journal of Chemical Sciences* **2015**, *127*, 241-255.
- [132] D. J. Scott, M. J. Fuchter, A. E. Ashley, "Designing effective 'frustrated Lewis pair' hydrogenation catalysts", *Chem. Soc. Rev.* **2017**, *46*, 5689-5700.
- [133] J. Paradies, "From structure to novel reactivity in frustrated Lewis pairs", *Coord. Chem. Rev.* **2019**, *380*, 170-183.
- [134] L. Greb, S. Tussing, B. Schirmer, P. Oña-Burgos, K. Kaupmees, M. Lökov, I. Leito, S. Grimme, J. Paradies, "Electronic effects of triarylphosphines in metal-free hydrogen activation: a kinetic and computational study", *Chem. Sci.* **2013**, *4*, 2788.
- [135] G. Wittig, G. Steinhoff, "Azatriptycene", *Angew. Chem. Int. Ed.* **1963**, *2*, 396-396.
- [136] C. Jongsma, J. P. de Kleijn, F. Bickelhaupt, "Phosphatriptycene", *Tetrahedron* **1974**, *30*, 3465-3469.

- [137] F. J. M. Freijee, C. H. Stam, "Arsatriptycene and phosphatriptycene", *Acta Crystallogr. A* **1980**, *36*, 1247-1249.
- [138] J. Kobayashi, T. Agou, T. Kawashima, "A novel and convenient synthetic route to a 9-phosphatriptycene and systematic comparisons of 9-phosphatriptycene derivatives", *Chem. Lett.* **2003**, *32*, 1144-1145.
- [139] T. Agou, J. Kobayashi, T. Kawashima, "Synthesis, structure, and reactivity of a symmetrically substituted 9-phosphatriptycene oxide and its derivatives", *Heteroat. Chem* **2004**, *15*, 437-446.
- [140] H. Tsuji, T. Inoue, Y. Kaneta, S. Sase, A. Kawachi, K. Tamao, "Synthesis, structure, and properties of 9-phospha-10-silatriptycenes and their derivatives", *Organometallics* **2006**, *25*, 6142-6148.
- [141] Y. Uchiyama, J. Sugimoto, M. Shibata, G. Yamamoto, Y. Mazaki, "Bromine adducts of 9,10-diheteratriptycene derivatives", *Bull. Chem. Soc. Jpn.* **2009**, *82*, 819-828.
- [142] S. Konishi, T. Iwai, M. Sawamura, "Synthesis, properties, and catalytic application of a triptycene-type borate-phosphine ligand", *Organometallics* **2018**, *37*, 1876-1883.
- [143] H. Ube, Y. Yasuda, H. Sato, M. Shionoya, "Metal-centred azaphosphatriptycene gear with a photo- and thermally driven mechanical switching function based on coordination isomerism", *Nature Communications* **2017**, *8*, 14296-14301.
- [144] L. Hu, D. Mahaut, N. Tumanov, J. Wouters, R. Robiette, G. Berionni, "Complementary synthetic approaches toward 9-phosphatriptycene and structure-reactivity investigations of its association with sterically hindered Lewis acids", *J. Org. Chem.* **2019**, *84*, 11268-11274.
- [145] S. E. Creutz, J. C. Peters, "Catalytic reduction of N₂ to NH₃ by an Fe-N₂ complex featuring a C-atom anchor", *J. Am. Chem. Soc.* **2014**, *136*, 1105-1115.
- [146] L. Hu, D. Mahaut, N. Tumanov, J. Wouters, L. Collard, R. Robiette, G. Berionni, "Sterically hindered *ortho*-substituted phosphatriptycenes as configurationally stable P-chirogenic triarylphosphines", *Dalton Trans.* **2021**, *50*, 4772-4777.
- [147] V. D. Vuković, E. Richmond, E. Wolf, J. Moran, "Catalytic Friedel-Crafts reactions of highly electronically deactivated benzylic alcohols", *Angew. Chem. Int. Ed.* **2017**, *56*, 3085-3089.
- [148] H. Mayr, J. Ammer, M. Baidya, B. Maji, T. A. Nigst, A. R. Ofial, T. Singer, "Scales of Lewis basicities toward C-centered Lewis acids (Carbocations)", *J. Am. Chem. Soc.* **2015**, *137*, 2580-2599.
- [149] G. Berionni, L. Hu, A. Ben Saïda, A. Chardon, M. Gama, A. Osi, D. Mahaut, X. Antognini Silva, "Opening up new research lines in Lewis acid/base catalysis", *Chimie Nouvelle* **2018**, *128*, 13-16.
- [150] D. Mahaut, G. Berionni, B. Champagne, "9-Phosphatriptycene derivatives: From their weak basicity to their application in frustrated Lewis pair chemistry", *J. Phys. Chem. A* **2022**, *126*, 2794-2801.
- [151] A. J. Poe, D. H. Farrar, Y. Zheng, "Systematic kinetics of high nuclearity metal carbonyl clusters. Associative substitution reactions of Ru₆C(CO)₁₇ with P-donor nucleophiles", *J. Am. Chem. Soc.* **1992**, *114*, 5146-5152.
- [152] K. Haav, J. Saame, A. Kütt, I. Leito, "Basicity of phosphanes and diphosphanes in acetonitrile", *Eur. J. Org. Chem.* **2012**, *2012*, 2167-2172.
- [153] D. Mahaut, B. Champagne, G. Berionni, "Frustrated Lewis pair-catalyzed hydrogenation of unactivated alkenes with sterically hindered 9-phosphatriptycenes", *ChemCatChem* **2022**, *14*, e202200294.

Nouvelles de la division des Jeunes Chimistes de la SRC

1. La journée de rencontre des Jeunes Chimistes de la SRC à l'ULiège (2022)




Les
Jeunes Chimistes
de la Société Royale de Chimie
vous convient à leur

JOURNÉE-RENCONTRE

14^e édition
Vendredi 1^{er} avril 2022

Bat. B8 - Campus Sart Tilman
Théâtre Dick Annegarn
ULiège

Infos et inscriptions:
www.facebook.com/JeunesChimistesSRC
ou
jeuneschimistesrc@gmail.com






Le 1^{er} avril 2022 marqua le retour tant attendu des activités des Jeunes Chimistes de la Société Royale de Chimie (SRC), au sein de l'université de Liège. Cette édition fut un véritable succès, mettant fin à deux années d'interruption due

à la crise sanitaire. Axée sur le thème de la «Communication Scientifique», cette journée de séminaires a réuni environ 100 jeunes chercheurs issus des 5 universités de la Fédération Wallonie-Bruxelles.

Parmi les participants, 10 doctorants ont eu l'opportunité de présenter leurs travaux de manière orale, tandis que 26 autres ont brillamment exposé leurs recherches à travers des posters captivants. En complément de ces présentations, le programme de la journée s'est enrichi de trois keynotes, dispensées par des éminents intervenants : Madame Aline Wilmet de l'UNamur, le Docteur David Homburg de l'ULiège et le Professeur Bernard Leyh, également de l'ULiège.

Ces trois experts ont habilement couvert une gamme complète de sujets liés à la communication scientifique, depuis l'évolution historique jusqu'aux meilleures pratiques à adopter pour des présentations percutantes. De plus, outre les distinctions décernées au meilleur poster et à la meilleure présentation, il convient de noter que cette manifestation a pu être proposée gratuitement, grâce au soutien financier du département de chimie de l'université de Liège, ainsi que des principales unités de recherche qui le composent, en plus du Comité de Gestion du Bulletin.



Photo de tous les participants à la Journée des Jeunes Chimistes de la SRC 2022, à l'université de Liège

2. Prise de relève du duo de Liège

En fin d'année 2022, Myriam Neuman, université de Namur, alors présidente du comité des Jeunes Chimistes de la SRC, a défendu sa thèse, libérant ainsi la présidence du comité. Le comité était alors principalement composé de jeunes chercheurs en fin de thèse, résultant de la difficulté de recruter des nouveaux membres durant la crise sanitaire. Une potentielle succession s'est alors naturellement tournée vers les nouvelles recrues de 2022 : malgré leur expérience plus réduite, ils ont en effet la capacité de représenter une solution plus durable pour garantir la bonne poursuite du comité. Après un vote unanime, Thibault Massenet et Max Larry, tous deux doctorants de l'université de Liège, ont été élus co-présidents du comité.

Depuis le début de 2023, Max et Thibault président donc le comité des Jeunes Chimistes de la SRC. Grâce à des contacts noués lors des événements de rencontre regroupant les doctorants en chimie des différentes universités de la Fédération Wallonie-

Bruxelles, les membres restants du comité sont arrivés à trouver des remplaçants pour tous les postes devenus vacants suite à des fins de thèse.



Le comité des Jeunes Chimistes de la SRC, avec de gauche à droite : Max Larry, Nicolas Callebaut, Thibault Massenet, Martin Blavier, Thomas Robert et Pierre Mathieu (David Cauwenbergh manque sur la photo)

Le poste de secrétaire est désormais assumé par Pierre Mathieu, jeune doctorant de l'université de

Mons. Un deuxième nouveau doctorant recruté à l'université de Mons, Thomas Robert, a accepté de devenir le nouveau trésorier après une période de transition où il sera encore épaulé par l'ancien trésorier, David Cauwenbergh. Finalement, le dernier poste vacant après le départ de l'équipe de Myriam Neuman, celui de responsable de la communication, est repris par Martin Blavier, jeune doctorant de l'université de Liège, et Nicolas Callebaut de l'université de Bruxelles qui l'épaulera pour sa dernière année de thèse.

Ce noyau de 7 personnes qui forme le comité assure le bon fonctionnement de la division des Jeunes Chimistes de la SRC. Les membres du comité construisent les équipes responsables de l'organisation des événements, se chargent des missions de partage de contacts et d'informations intéressantes envers leurs membres, assument les tâches de réseautage, et accomplissent les tâches administratives liées à une telle organisation.

3. Young Chemists' day de la SRC à l'Université de Mons (2023)

Le 22 mai 2023 s'est déroulée la journée des Jeunes Chimistes de la SRC à l'université de Mons. Cette journée, placée sous le thème de l'apport de la modélisation et de la chimie quantique à la recherche, était une opportunité pour tout jeune chercheur de partager ses travaux et présenter ses résultats, le tout dans un cadre moins intimidant que des conférences scientifiques.

Malgré la spécificité du sujet, la journée a attiré une soixantaine de jeunes chimistes venant d'horizons divers : d'abord de la Fédération Wallonie-Bruxelles, mais également de France, de Roumanie et même du Burkina Faso.

La journée a été ponctuée par trois présentations d'experts dans le domaine de la chimie quantique ou théorique. Ces trois experts furent le Pr. David Beljonne de l'université de Mons, spécialiste dans la modélisation des phénomènes opto-électroniques



Photo de tous les participants de la Journée des Jeunes Chimistes de la SRC 2023, à l'université de Mons

dans des matériaux organiques, le Pr. Benoît Champagne de l'université de Namur, spécialisé en chimie théorique et ses applications pour décrire les phénomènes d'optique non linéaire, et le Dr. Andrea Minoia de l'université de Mons, s'intéressant à l'élaboration de modèles multi-échelles afin d'étudier des interfaces moléculaires complexes. Accompagnant ces trois présentations thématiques d'une grande qualité, 11 courtes présentations orales de leurs travaux ont été données par des jeunes chimistes. Toutes les disciplines étaient alors à l'honneur, passant de la chimie théorique à la chimie organométallique, en passant par la chimie inorganique et la chimie analytique.

Une session de présentation de posters a également eu lieu, ce fut l'occasion de découvrir la recherche s'effectuant ailleurs dans la Fédération Wallonie-Bruxelles. Le cadre très convivial de cette journée a permis le dialogue direct entre 27 jeunes chercheurs motivés et leur public, dans une atmosphère détendue. Durant cette session, chacun était libre de désigner ses trois posters favoris parmi ceux présentés, en vue de décerner le prix du meilleur poster à celui qui aurait récolté le plus de voix. Le prix de la meilleure présentation orale, quant à lui, a été remis sur concertation des membres du comité organisateur et des trois experts.

La remise des prix a eu lieu en fin de journée ; ils ont été décernés par le Pr. Philippe Leclere, représentant l'Institut des Matériaux de l'UMONS, un des principaux sponsors de cette journée. Le prix de la meilleure présentation est revenu à

Manuel Cardoso, doctorant à l'ULiège. Le prix du meilleur poster est quant à lui resté à domicile, revenant à Louis Groignet, doctorant à l'UMONS. Toutes nos félicitations aux deux lauréats !

Cette journée a constitué une belle expérience pour les jeunes chimistes qui y ont participé. Elle a donné un aperçu à toutes les personnes présentes de la recherche qui est menée en Fédération Wallonie-Bruxelles, en plus de leur permettre de développer leur carnet d'adresses. Il convient de noter que le succès de cet événement n'aurait pas pu être atteint sans le soutien financier du département de chimie de l'UMONS et de l'Institut des Matériaux, ainsi que du Comité de Gestion du Bulletin.

4. Note de fin

Étant une association dépendant de l'aide de volontaires, le comité des jeunes chimistes de la SRC est à la recherche permanente de doctorant.e.s intéressé.e.s qui souhaiteraient faire partie de ce sous-groupe dynamique de la SRC. Tout.e jeune chercheur.euse est le.a bienvenu.e - dès que son domaine de recherche touche à la chimie - dans cette structure pour créer des nouveaux contacts, faire du réseautage, partager ses découvertes ou simplement discuter avec des pairs. En cas d'intérêt, n'hésitez pas à contacter les responsables de l'association via l'adresse mail jeuneschimistessrc@gmail.com, via leur page Facebook (Jeunes Chimistes de la SRC) ou même via LinkedIn (Jeunes Chimistes SRC).



Manuel Cardoso, doctorant à l'ULiège



Louis Groignet, doctorant à l'UMONS

Echos de la Journée scientifique de la SRC 2023

La Journée scientifique annuelle de la SRC s'est déroulée le 19 Octobre 2023 à l'UCLouvain sur le thème 'Photochemistry, a shining tool for scientist'. Elle a rassemblé 135 participants. Son programme comprenait 4 conférences plénières [Dr. KERLIDOU-CHAVAROT Murielle (CEA

Grenoble), Prof. WENGER Oliver (Universität Basel), Prof. MEYER Gerald (University of North Carolina at Chapel Hill), Prof. QUINN Susan (University College Dublin)], 4 communications par les lauréats des prix SRC et une séance de communications par affiche (34).



Remise des prix SRC et Solvay

La SRC a un nouveau logo...

SRC
SOCIÉTÉ ROYALE DE CHIMIE

Pour vous faire membre de la SRC et accéder gratuitement à la revue Chimie Nouvelle :

il vous suffit de verser au compte BNP Paribas Fortis : BE60 2100 4208 0470
la somme indiquée dans le tableau ci-dessous :

Membres résidant en Belgique et au Luxembourg

Membres effectifs : **50 euros**

- participation gratuite ou à prix réduit à toutes les activités de la SRC
- abonnement gratuit à la revue "Chimie Nouvelle"
- accès gratuit à la bibliothèque de la SRC.

Membres associés : **25 euros**

- réservé, avec les mêmes avantages que les membres effectifs, aux jeunes diplômés du deuxième cycle pendant deux ans, aux professeurs de l'enseignement secondaire et aux retraités.

Membres Juniors : Gratuit

- réservé aux étudiants de dernière année du 2^e cycle universitaire (2^e master), des Ecoles d'Ingénieurs industriels et des graduats en Chimie et Biochimie avec les mêmes avantages que les membres effectifs.

Demandeurs d'emploi : **15 euros**

- mêmes avantages que les membres effectifs + insertion gratuite dans Chimie Nouvelle d'une annonce de demande d'emploi.

Membres résidant à l'étranger

Membres effectifs : **60 euros**

Membres associés : **35 euros**